

QUANTUM FIELDS AND FUNDAMENTAL FORCES

---

The Causal Ladder and the  
Causal Set Approach to  
Quantum Gravity

---

*Author:*  
Ibrahim HAJAR

*Supervisor:*  
Dr. Fay DOWKER

September 22, 2022

Imperial College  
London

## Abstract

In this paper we present an examination of the hierarchy of causal restrictions one may impose on spacetime, known as the causal ladder. Our goal is to give a precise context to and formulation of the central conjecture of Causal Set Theory, by situating the conjecture in the framework of the causal ladder. We begin by tracing historical work concerning the two central notions of Causal Set Theory – spacetime discreteness, and causality. We then unpack the causal ladder, and some of E. Minguzzi’s accompanying terminology concerning causal relations on a set (which could be a spacetime). We then give motivations to explore the interface of causality and geometry based on results of Hawking and Penrose. Key theorems of Hawking are then situated before entering the arena of Causal Set Theory itself, and its central conjecture. In order to move toward either a proof or a precise statement of the central conjecture, we examine spacetimes with specific causal structures. We then undertake Poisson sprinklings in three specific spacetimes. After observing the sorts of causal sets which can be faithfully embedded in these spacetimes, we consider work by Luca Bombelli and Johan Noldus in analyzing the approximate geometries of Lorentzian manifolds. With information on the causal sets and approximate geometries of the three sample spacetimes, we answer the question of whether they pose a contradiction to the central conjecture. An ultimate proof of the conjecture will rely on a precise reformulation of the conjecture. We assess work by Bombelli and Noldus on approximate isometries to help us build a more precise understanding of the conjecture.

# Contents

<b>1</b>	<b>Historical Threads of Causal Set Theory</b>	<b>3</b>
1.1	Discreteness . . . . .	3
1.2	Causality . . . . .	5
<b>2</b>	<b>A Hierarchy of Causal Restrictions</b>	<b>8</b>
2.1	Foundations of Causal Structure . . . . .	8
2.2	Minguzzi and Abstract Relations . . . . .	13
2.3	The Causal Ladder . . . . .	14
2.3.1	Alternative Characterizations of Two Rungs . . . . .	16
<b>3</b>	<b>Undergirdings for the Relationship between Causality and the Structure of Spacetime</b>	<b>18</b>
3.1	Causality and Conformal Geometry . . . . .	18
3.2	Causality and Topology . . . . .	20
3.2.1	Topological Basics . . . . .	20
3.2.2	Causal Topology and a New Characterization of Strong Causality . . . . .	21
<b>4</b>	<b>Building up to the Central Conjecture of Causal Set Theory</b>	<b>27</b>
4.1	Three Key Theorems of Hawking . . . . .	27
4.2	The Hauptvermutung of Causal Set Theory . . . . .	30
<b>5</b>	<b>Obtaining Faithful Embeddings: Poisson Processes</b>	<b>32</b>
<b>6</b>	<b>Analyzing Causal Peculiarities</b>	<b>36</b>
6.1	Past but Not Future-Distinguishing . . . . .	36
6.2	Distinguishing but Not Strongly Causal . . . . .	40
6.3	Strongly Causal but Not Globally Hyperbolic . . . . .	43
<b>7</b>	<b>Three Spacetimes and Two Causal Sets</b>	<b>44</b>
7.1	Locating $\mathcal{M}_1$ , $\mathcal{M}_2$ , and $\mathcal{M}_3$ on the Causal Ladder . . . . .	46
7.2	Poisson Sprinklings in the Three Diamonds . . . . .	47
7.2.1	Sprinkling in $\mathcal{M}_1$ . . . . .	49
7.2.2	Sprinkling in $\mathcal{M}_2$ . . . . .	53

7.2.3	Sprinkling in $\mathcal{M}_3$ . . . . .	56
7.2.4	The Probability of a Blocked Relation . . . . .	61
<b>8</b>	<b>Toward Identifying Essential Uniqueness</b>	<b>68</b>
8.1	$\epsilon$ -Isometries . . . . .	69
8.2	A Lorentzian Generalization of Euclidean Isometries . . . . .	70
<b>9</b>	<b>Conclusions and Future Work</b>	<b>74</b>

# Chapter 1

## Historical Threads of Causal Set Theory

While Causal Set Theory aims to be a quantum theory of gravity, it might be more immediately described as a quantum theory of spacetime itself. Causal Set Theory posits that spacetime can be fully characterized by two fundamental features: causality and discreteness. The causality and discreteness of Causal Set Theory ask that a spacetime satisfy very minimal structural conditions, from which the suite of features experienced and used in General Relativity can be derived.

We will start by tracing historical threads of discreteness and causality in recent work. In the twentieth century, these two notions were often tackled independently of one another. Discretization of spacetime was explored as a means to mitigate divergences arising in quantum theories, and causality was initially addressed as a means of reproducing the familiar geometric aspects and symmetry groups associated to spacetime. Accordingly, we describe these histories disjointly before finding their logical conjunction in the foundational work of Stephen Hawking and others.

### 1.1 Discreteness

After the success of quantum theory, discreteness appeared to be a central tenet of fundamental physics. The discreteness at play in early quantum theories often appeared through integer-labeled eigenvalues of an observable promoted to operator. For this reason, we refer to this as discretization, an active verb, rather than the discreteness of eventual Causal Set Theory, which refers to a latent but fundamental and ever-present feature of spacetime which, once uncovered, should reproduce the familiar continuum.

In 1946, Hartland Snyder proposed promoting the elements of spacetime tuples,  $(x, y, z, t)$ , from continuous coordinates to Hermitian operators [1]. These operators had discrete spectra, the linear combinations of which left the Lorentzian

bilinear invariant. Snyder went about reproducing spatial and momentum commutation relations, and arrived at the conclusion that this approach, while being invariant with respect to Lorentz transformations that leave the origin fixed, did not allow for symmetry under the full Lorentz group. In fact, from the start, promoting the event-points to operators required selecting a particular frame.

Two years later, Alfred Schild took an approach to discretization which latticized space [2]. Accordingly, he considered only spacetime events whose  $(x, y, z, t)$  coordinates were integers. Motivated by renormalizing the self-energy of the electron, Schild chose as the fundamental length between lattice points, the classical electron radius. This can be contrasted later on with the minimal length scale used in Causal Set Theory – the Planck Length.

In Schild’s framework, the path of a particle consists of “temporally ordered lattice points” joined by either timelike or null lines. Schild utilized methods of discrete mathematics and number theory to discretize spacetime. Points in Schild’s spacetime lattice were modeled by the Gaussian integers,  $\mathbf{Z}[i] = \{a + ib | a, b \in \mathbb{Z}\}$ . By importing the properties of integral domains (the discrete ring structure formed by the Gaussian integers), Schild deduced that the Lorentz transformations which left his lattice invariant, termed “integral Lorentz transformations,” were dense in the Lorentz group.

While Schild’s symmetry group was dense in the Lorentz group, it was not itself the full Lorentz group. In addition to this incomplete symmetry, the timelike lines which described the motion of matter, revealed a minimum speed of .86 times the speed of light, which was too large to be physical.

In 1955, E.L. Hill attempted to continue Snyder’s work by searching for a discretized spacetime which was, again, invariant under only a dense subgroup of the full Lorentz group [3]. He did this by examining Lorentz transformations with rational coefficients (since  $\mathbb{Q}$  is dense in  $\mathbb{R}$ ), continuing in the number theoretic spirit of Snyder. This approach did allow Hill to avoid Schild’s problem of an exorbitantly high minimal velocity parameter. However, he ran into a familiar problem: symmetry under a significantly restricted subgroup of the Lorentz group which did not extend to the full group. In particular, Hill recognized that there may well be representations of the discrete (though dense) subgroup he was considering, which would be disallowed by the full Lorentz group.

These attempts largely followed closely in the spirit of quantum theory, by discretizing classically continuous observable quantities, and considering their integer or rational number-labeled spectra. The discreteness at work in Causal Set Theory, as we will outline, exists at a kinematic level, and reveals vital information about the geometry of spacetime. Given that Causal Set Theory aims to give a quantum description to gravity – a force currently best understood in a continuous space – we are faced with the challenge of reconciling the discrete with the continuous. This juncture is hastened by examining causality, which was the element missing from the work we just outlined. We describe this thread next.

## 1.2 Causality

Given the daunting aim of uniting the discrete and the continuous, it is heartening to learn from the father of the continuum, Bernhard Riemann. Riemann's work on the theory of manifolds – mostly in a continuous, and furthermore, a differentiable setting – was the mathematical antecedent for Einstein's General Relativity. Yet Riemann himself had doubts about the validity of his geometries to describe space in the infinitely small (space was often the word he used, before Minkowski's mathematical and linguistic conjunction of space and time).

While Riemann contented himself with geodesic extensions and limiting processes to describe what he called the “infinitely great,” he was less at ease with contemporary understanding of the infinitely small. In a Nature article published his death, Riemann felt himself

“quite at liberty to suppose that the metric relations of space in the infinitely small do not conform to the hypotheses of geometry; and we ought in fact to suppose it, if we can thereby obtain a simpler explanation of phenomena.”

With great prescience, he pondered a link between discrete length scales and causality, positing that

“it is upon the exactness with which we follow phenomena into the infinitely small that our knowledge of their causal relations essentially depends.” [4]

He went on to compare the extraction of causal information from the discrete to the way in which classical mechanics was built upon calculus of the infinitesimally small. Riemann concludes that the infinitely small, and the novel geometric description it must carry, will be of utmost physical significance.

As we foray into causal analysis, the most basic definition we require is that of a partially ordered set. In what follows, although  $\mathcal{M}$  may be interpreted as a spacetime, the following definition requires that  $\mathcal{M}$  be only a set, not that it have any structure, continuous or otherwise.

**Definition 1.** *The double  $(\mathcal{M}, <)$  is a reflexive partially ordered set if the relation  $<$  satisfies*

- *acyclicity:*  $\forall x, y \in \mathcal{M}$  if  $x < y$  and  $y < x$  then  $x = y$
- *reflexivity:*  $\forall x \in \mathcal{M}, x < x$
- *transitivity:*  $\forall x, y, z \in \mathcal{M}$  if  $x < y$  and  $y < z$  then  $x < z$ .

For clarity and future use we give the definition of an irreflexive partially ordered set as well.

**Definition 2.** *The double  $(\mathcal{M}, <<)$  is an irreflexive partially ordered set if the relation  $<<$  satisfies*

- *asymmetry:*  $\forall x, y \in \mathcal{M}$ , if  $x << y$ , then we do not have  $y << x$
- *irreflexivity:*  $\forall x \in \mathcal{M}$ , we do not have  $x << x$
- *transitivity:*  $\forall x, y, z \in \mathcal{M}$  if  $x << y$  and  $y << z$  then  $x << z$ .

In 1914, Alfred Robb set out to “show that spacial relations may be analyzed in terms of the time relations of *before* and *after*” [5]. In his “A Theory of Space and Time”, Robb set out 21 postulates which helped him build up a geometry on Minkowski space. He constructed an irreflexive partial order using the “time” relation between what he called “instants”, and delivered results modeled after well-known Euclidean geometry. His culminating theorem gave an analogue of the Archimedean property for the real numbers. Robb’s final postulate was a Lorentzian version of the axiom of Dedekind. For statements of these well-known Euclidean results one can see for example, [6].

In 1966, E.H. Kronheimer and Roger Penrose defined an abstract causal space axiomatically [7]. Their construction makes use of a set with two partial orderings, and without any requirements on the structure of the set.

We first recall the two partial orderings used by Kronheimer and Penrose, which will be of central importance throughout this paper. Given a set  $X$  and elements  $x, y \in X$  then we write  $x < y$  to denote  $x$  being in the *causal past* of  $y$ . The partial order given by  $<$  is reflexive in line with Definition 1. There is also an irreflexive partial order denoted by  $<<$ . We write  $x << y$  if  $x$  is in the *chronological past* of  $y$ .

For the moment, the names given to the partial orders  $<$  and  $<<$  hold a somewhat abstract physical significance, wherein points contained in a partial order constitute events which may communicate with each other, via either light or matter. A precise definition in terms of temporally oriented curves will be given in the next chapter. Kronheimer and Penrose also used the term *horismos* if  $x$  and  $y$  are causally, but not chronologically related. This term is necessary because the causal relation encompasses more points than the chronological relation. Indeed the chronologically related points are a subset of the causally related ones. The horismotic relation denotes events which can only communicate via light, while causal relations include events which may be related by the travel of matter as well. For horismotically related points  $x$  and  $y$ , where  $x < y$  but not  $x << y$ , we write  $x \rightarrow y$ . Given these three *causal relations*, and a set  $X$ , we have the following definition.

**Definition 3.** [7] *An abstract causal space is a quadruple  $(X, <, <<, \rightarrow)$  where the three causal relations satisfy the following axioms, for all  $x, y, z \in X$ :*

1.  $x < x$
2. if  $x < y$  and  $y < z$ , then  $x < z$
3. if  $x < y$  and  $y < x$ , then  $x = y$
4. not  $x << x$
5. if  $x << y$  then  $x < y$
6. if  $x < y$  and  $y << z$ , then  $x << z$
7.  $x << y$  and  $y < z$ , then  $x << z$



8.  $x \rightarrow y$  if and only if  $x < y$  and not  $x \ll y$ .

We note that axioms (1) to (7) imply the reflexive partial ordering formed by the causal relation and the irreflexive partial ordering formed by the chronological relation. Conditions (6) and (7) give us a “mixed transitivity condition.” In a continuous setting, these two conditions do not need to be promoted to axioms, but can be derived using a construction involving continuous curves and particular classes of neighborhoods. This will be proven in chapter 2.

Two years earlier, E.C. Zeeman had used the chronological relation on Minkowski space to recover the group generated by inhomogeneous Lorentz transformations together with dilatations (the homothety group) [8]. Zeeman’s work does require the set previously called  $X$  to have a continuous structure, but his results concern the physicality of spacetime, so this is sensible requirement.

Central to Zeeman’s work is a map called a chronological automorphism, which is an automorphism preserving the chronological ordering of points in  $\mathbb{M}^d$ . That is,

**Definition 4.** *Given an automorphism,  $f : \mathbb{M}^d \rightarrow \mathbb{M}^d$ ,  $f$  is a chronological automorphism if,  $\forall x, y \in \mathbb{M}^d$ :*

$$x \ll y \iff f(x) \ll f(y).$$

In his work, Zeeman proves that the group of chronological automorphisms on  $d$ -dimensional Minkowski space is isomorphic to the homothety group, if the dimension is greater than two. Zeeman’s 1964 result, which identifies chronological isomorphisms with the homothety group on Minkowski space provided the title of his landmark paper, “Causality implies the Lorentz Group.” By starting from only the partial order generated by the chronological relation on a spacetime, Zeeman was able to recover the required symmetry group of  $\mathbb{M}^d$ .

The causal, chronological, and horismotic relations have been referenced in this section. There is in fact, an entire hierarchy of causal restrictions which we may ask a spacetime to satisfy. These restrictions, as we will see, are conditions on how the elements of a spacetime are allowed to be related to each other via the causal and chronological relations.

## Chapter 2

# A Hierarchy of Causal Restrictions

In this chapter, we build up to an analysis of the causal ladder, a term coined by Minguzzi [9], which refers to a sequence of increasingly restrictive conditions regarding the causal structure of spacetime.

Our analysis of the causal ladder will move between causal, geometric, and topological description which requires us to set some foundational definitions.

### 2.1 Foundations of Causal Structure

**Definition 5.** A  $C^n$   $d$ -dimensional manifold  $\mathcal{M}$  is a set with a  $C^n$  atlas  $\{\mathcal{U}_\alpha, \phi_\alpha\}_{\alpha \in \mathbb{N}}$ , where  $\forall \alpha, \mathcal{U}_\alpha \subseteq \mathcal{M}$  and  $\phi_\alpha : \mathcal{U}_\alpha \rightarrow \mathbb{R}^d$  are injections with  $\phi_\alpha(\mathcal{U}_\alpha)$  open in  $\mathbb{R}^d$ .

The atlas must satisfy:

1.  $\mathcal{M} = \bigcup_\alpha \mathcal{U}_\alpha$
2.  $\forall \alpha, \beta$  if  $\mathcal{U}_\alpha \cap \mathcal{U}_\beta \neq \emptyset$ , then the transition map given by  $\phi_\alpha \circ \phi_\beta^{-1} : \phi_\beta(\mathcal{U}_\alpha \cap \mathcal{U}_\beta) \rightarrow \phi_\alpha(\mathcal{U}_\alpha \cap \mathcal{U}_\beta)$  is a  $C^n$  mapping between open subsets of  $\mathbb{R}^d$ .

**Definition 6.** A  $C^n$  metric  $g_{\mu\nu}$  at a point  $p \in M$  is a  $C^n$  symmetric  $(0,2)$ -tensor.

**Definition 7.** The signature of a metric  $g_{\mu\nu}$  at  $p \in M$  is the number of positive eigenvalues of the matrix  $g_{\mu\nu}$  at  $p$  minus the number of negative eigenvalues at  $p$ .

If the matrix  $g_{\mu\nu}$  is invertible and continuous, then the signature of  $g_{\mu\nu}$  is constant on  $M$ , and using a suitable basis for  $M$  the metric can be written as

$$g_{\mu\nu} = \text{diag}(+1, \dots, +1, -1, \dots, -1)$$

with a  $+1$  for every positive eigenvalue and a  $-1$  for every negative eigenvalue.

**Definition 8.** A metric whose signature is  $d - 2$  is a Lorentz metric, which is usually given in the form

$$g_{\mu\nu} = \text{diag}(-1, +1, \dots, +1, ),$$

with 1 negative eigenvalue and  $d - 1$  positive eigenvalues.

**Definition 9.** A Lorentz metric  $g_{\mu\nu}$  allows for the classification of a vector  $v$  in the tangent space  $T_p\mathcal{M} \forall p \in \mathcal{M}$  according to the sign of  $v^\mu v^\nu g_{\mu\nu} = v^2$ . Using the signature given in Definition 14, we have

- $v^\mu$  is timelike if  $v^2 < 0$
- $v^\mu$  is null if  $v^2 = 0$
- $v^\mu$  is spacelike if  $v^2 > 0$

A vector which is either timelike or null is said to be causal.

**Definition 10.** A time orientation is a causal vector field  $t^\mu$  defined on  $\mathcal{M}$ . A manifold which admits a time orientation is said to be time orientable.

**Definition 11.** Given a time orientation  $t^\mu$  on  $\mathcal{M}$ , a causal vector  $v^\nu$  is future-directed if  $t^\mu v^\nu g_{\mu\nu} \leq 0$ .  $v^\nu$  is past-directed if  $t^\mu v^\nu g_{\mu\nu} > 0$ .

We have an analogous definition for past directed causal vectors.

**Definition 12.** Given subsets  $A, B \subseteq \mathcal{M}$ , the causal future of  $A$  relative to  $B$  is the set  $J^+(A, B)$ , consisting of the union of  $A \cap B$  with all points in  $B$  which can be reached by a future-directed causal curve starting in  $A$ .

**Definition 13.** Given subsets  $A, B \subseteq \mathcal{M}$ , the chronological future of  $A$  relative to  $B$ , denoted by  $I^+(A, B)$ , is the set of points in  $B$  which can be reached by a future-directed chronological curve starting in  $A$ .

**Definition 14.** Given subsets  $A, B \subseteq \mathcal{M}$ , the future horismos of  $A$  relative to  $B$  denoted by  $E^+(A, B)$  is the set of points in  $B$  which can be reached by a future-directed null curve starting in  $A$ .  $E^+(A)$  can be equivalently defined as  $J^+(A) - I^+(A)$ .

The sets  $J^-(A, B)$ ,  $I^-(A, B)$ , and  $E^-(A, B)$  denote the analogous past causal, chronological, and horismos of  $A$  relative to  $B$ . When  $B = \mathcal{M}$  in the above definitions, ie the entire spacetime, we write  $J^-(A)$ , instead of  $J^-(A, \mathcal{M})$ , and similarly for the chronological and horismos sets. When  $A$  consists of a single point,  $A = \{p\} \in \mathcal{M}$ , we write  $J^-(p)$ ,  $I^-(p)$ , and  $E^-(p)$ .

Let us also define important classes of neighborhoods which may be defined around a particular point,  $x$  in a spacetime,  $\mathcal{M}$ .

**Definition 15.** A neighborhood  $U$  of  $x$  is a future locality neighborhood if every future-directed causal curve from  $x$  intersects  $U$  in a connected set.

We can define a past locality neighborhood similarly.

Before defining our next class of neighborhood, we require the following map.

**Definition 16.** *Take a point  $p \in \mathcal{M}$  and  $v \in T_p\mathcal{M}$ . Then consider an affinely parameterized geodesic,  $\gamma(\lambda) \subseteq \mathcal{M}$ , such that  $\gamma(0) = p$  and  $\gamma'(0) = v$ . Then the exponential map is a  $C^\infty$  map,*

$$\begin{aligned} \exp_p(v) : T_p\mathcal{M} &\longrightarrow \mathcal{M} \\ v &\longmapsto q \end{aligned}$$

where  $\gamma(1) = q$ .

**Definition 17.** *A normal neighborhood  $N$  of  $x$  is one in which the exponential map is a diffeomorphism from the origin in Minkowski space to  $N$ .*

**Definition 18.** *A normal neighborhood  $N$  of  $x$  is said to be simply convex if  $N$  is not only a normal neighborhood of  $x$ , but also a normal neighborhood of every other point  $y \in N$ .*

A simply convex neighborhood,  $N$  has the key property that any two points,  $q, r \in N$  can be joined by a geodesic which is unique up to reparametrization, whose endpoints are  $q$  and  $r$  and is completely contained in  $N$ .

**Definition 19.** *A simple region,  $N$  is a simply convex open subset of the spacetime  $\mathcal{M}$  such that the closure of  $N$ ,  $\overline{N}$  is compact and contained in a simply convex open set.*

**Definition 20.** *An open subset  $N \subseteq \mathcal{M}$  is causally convex if no future-directed timelike geodesic intersects  $N$  in a disconnected set.*

**Definition 21.** *A causally convex open set whose closure is contained in a simple region (which is also contained in the spacetime), is a local causality neighborhood.*

We now present a proposition giving conditions for two points to be chronologically related in the mixed transitivity fashion of Kronheimer and Penrose. Before this, we require one lemma, which is presented without proof.

**Lemma 2.1.1.** *[10] Let  $N$  be a simple region. Suppose that  $a, b, c \in \overline{N}$  and that the geodesics joining  $a$  to  $b$  and  $b$  to  $c$  are both future-causal. Suppose further that one of the following is true: (1) the two geodesics have distinct directions at  $b$  if both geodesics are null, or (2) there exists a causal curve  $\gamma \subset \overline{N}$  joining  $a$  to  $c$ . Then the geodesic joining  $a$  to  $c$  is future-timelike.*

**Proposition 2.1.2.** *[10] Let  $a, b, c, \in \mathcal{M}$ . Then either of the following two conditions,*

- $a \in I^-(b)$  and  $b \in J^-(c)$
- $a \in J^-(b)$  and  $b \in I^-(c)$

imply that  $a \in I^-(c)$ .

We note that this proposition was promoted to an axiom in Kronheimer and Penrose's definition of an abstract causal space. In a continuous setting, however, it can be proven from more basic principles.

*Proof.* We present a proof that the first condition above yields the desired implication, with the proof based on the second condition being analogous.

Let  $\alpha$  be a timelike curve joining  $a$  to  $b$ , and  $\gamma$  be a causal curve joining  $b$  to  $c$ . We assume without loss of generality that no part of  $\gamma$  forms a closed loop. Also, since  $\gamma$  is compact, it can be covered by a finite number of simple regions  $N_1, \dots, N_r$ .

Set  $b = x_0 \in N_{i_0}$ , where the subscript on  $i$  refers to the fact that this is not necessarily the  $0^{\text{th}}$  neighborhood in the finite covering, but any neighborhood we pick in the following construction which contains the point  $x_0$ . Let  $x_1$  be the future endpoint of the connected component of  $\gamma \cap \overline{N_{i_0}}$  which begins at  $x_0$ . Choose  $y_1 \in N_{i_0}$  with  $y_1 \neq x_0$ . Then by Lemma 2.1.1, the geodesic joining  $x_1$  to  $y_1$  is future-timelike. Now if  $x_1 = c$ , then the proof is complete.

If  $x_1 \neq c$ , then  $x_1 \notin N_{i_0}$  and we say  $x_1 \in N_{i_1}$ . In this case, let  $x_2$  be the future endpoint of the connected component of  $\gamma \cap \overline{N_{i_1}}$  which begins at  $x_1$ . Choose  $y_2 \in N_{i_1}$ , on the geodesic joining  $x_1$  to  $y_1$  (and  $y_1 \neq x_1$ ). Then if  $x_2 = c$ , we are done.

If  $x_2 \neq c$ , then we repeat this argument. The process will terminate after a finite number of iterations because there is only a finite number of simple regions.  $\square$

We also include an illustration of this proof in Figure 2.1 below.

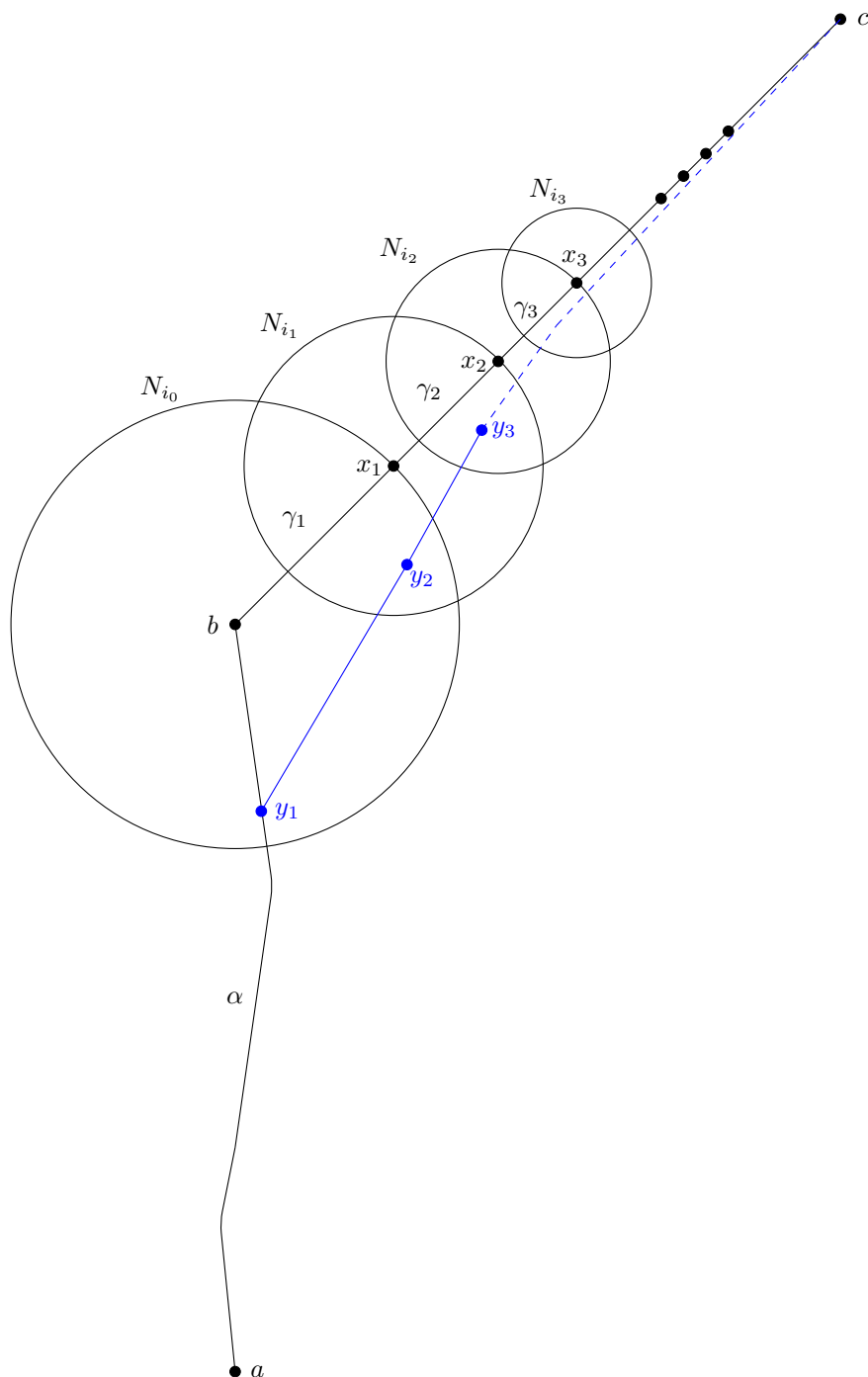


Figure 2.1: In this figure we visualize the curve  $\alpha$  joining  $a$  to  $b$  and the compact curve  $\gamma$  joining  $b$  to  $c$ . The simple regions covering  $\gamma$  are also included, containing the appropriate endpoints of the segments of  $\gamma$ . The blue curve represents the constructed timelike path beginning on the final segment of  $\alpha$  to the point  $c$ . It is assumed in this image that none of the  $x_1, x_2, \dots$  are themselves equal to  $c$ , and that the process outlined in the proof above iterates a finite number of times until  $c$  is reached.

We conclude this section with a proof that will be important in our later discussion of topology.

**Claim 1.** [10]  $I^+(p)$  is open  $\forall p \in M$

*Proof.* We show that we can place an open neighborhood around any element  $x \in I^+(p)$ .

$x \in I^+(p) \Rightarrow \exists \gamma(\lambda)$ , where  $\gamma(\lambda)$  is a timelike geodesic with endpoints at  $p$  and  $x$ . Suppose  $x \in N$  a simple region, and let  $y \neq x \in N$ .

Define  $Q := \{v \in \text{exp}_y^{-1}[N] \mid v \text{ timelike, future-directed}\}$ .

Then  $Q$  is open and  $\text{exp}_y^{-1}(x) \in Q$ . Since  $Q$  is open and  $\text{exp}_y[Q]$  is a homeomorphism,  $\text{exp}_y^{-1}[Q]$  is continuous, and we have that  $\text{exp}_y[Q]$  is an open set in  $\mathcal{M}$  and  $x \in \text{exp}_y[Q] \subseteq I^+(y) \subseteq I^+(p)$ .  $\square$

## 2.2 Minguzzi and Abstract Relations

Here we take the opportunity to introduce an abstract conceptualization of relations which stems from the notion of a relation on the direct product of a set with itself. This framework is developed by Minguzzi in [9] and [11], and will help us to describe rungs of the causal ladder later in this section.

In the following we take  $M$  to be simply a set.

**Definition 22.** A relation,  $R^+$  is a subset of  $M \times M$ .

**Definition 23.** Given  $I^+ = \{(p, q) \mid p \ll q\}$ ,  $R^+$  is a causal relation if  $I^+ \subset R^+$ .

We can recast the notions of reflexivity and antisymmetry as follows:

**Definition 24.** A relation  $R^+$  is reflexive if  $(x, x) \in R^+ \forall x \in M$ .  
A relation  $R^+$  for which  $(x, x) \notin R^+ \forall x \in M$  is irreflexive.

**Definition 25.** A relation  $R^+$  is antisymmetric if  $(x, z) \in R^+$  and  $(z, x) \in R^+$  together imply  $x = z$ .

**Definition 26.** The composition of two relations,  $R_1^+$  and  $R_2^+$  is given by  $R_2^+ \circ R_1^+ = \{(x, z) \in M \times M \mid (x, y) \in R_1^+ \text{ and } (y, z) \in R_2^+ \text{ for some } y \in M\}$ .

**Definition 27.** A relation  $R^+$  is transitive if  $R^+ \circ R^+ \subset R^+$ .

We can recast a partial order according to Minguzzi's framework.

**Definition 28.** A relation which is reflexive, transitive, and antisymmetric, is a (reflexive) partial order.

**Definition 29.** Given  $B^+ \subset R^+$ ,  $B^+$  is an  $R^+$ -ideal if  $B^+ \circ R^+ \subset B^+$  and  $R^+ \circ B^+ \subset B^+$ .

An abstract causal space in the sense of Kronheimer and Penrose can now be given by the triple  $(M, R^+, B^+)$  where  $R^+$  is a reflexive partial order, and  $B^+$  is an irreflexive  $R^+$ -ideal.

We also have

$$\begin{aligned} R^+(x) &:= \{y \in M \mid (x, y) \in R^+\}, \\ R^-(x) &:= \{y \in M \mid (y, x) \in R^+\}. \end{aligned}$$

Then,

$$y \in R^+(x) \iff (x, y) \in R^+ \iff x \in R^-(y).$$

We write  $R^+(x, y)$  for the set  $R^+(x) \cap R^-(y)$ .

**Definition 30.** *R-causality holds at  $x \in M$  if there is no  $z \in M$  such that  $(x, z) \in R^+$  and  $(z, x) \in R^+$ .*

*I-causality and J-causality are chronology and causality respectively.*

We next introduce the notion of future and past-distinguishing. This is our first introduction to a rung on the causal ladder. It will be situated in the causal hierarchy in the next section.

**Definition 31.** *A set is future-distinguishing if  $I^+(x) = I^+(y)$  implies  $x = y$ . Similarly, a set is past-distinguishing if  $I^-(x) = I^-(y)$  implies  $x = y$ . A set which is both future and past-distinguishing is said to be distinguishing.*

We can also give the notion of strong causality, another rung in the causal ladder. First we must dress the definition of a convex neighborhood in Minguzzi's terminology.

**Definition 32.** *A set  $U \subset M$  is R-convex if the causal relation  $R^+$  is such that  $\forall x, y \in U, R^+(x, y) \subset U$ .*

Then *J-convexity* is causal convexity as defined before.

**Definition 33.** *Strong R-causality holds at  $x \in M$  if  $x$  is contained in arbitrarily small R-convex neighborhoods. That is to say, for any neighborhood  $U$  containing  $x$ , there is an R-convex neighborhood  $V$  contained in  $U$  of which  $x$  is also an element, that is  $x \in V \subset U$ . A entire set is strongly R-causal if strong R-causality holds at every point of the set.*

Strong *J-causality* is strong causality.

## 2.3 The Causal Ladder

The causal ladder refers to a hierarchy of restrictions on the causal structure one may impose on a spacetime. This hierarchy can be listed in the fashion depicted below in Figure 2.2 with the strength of the restriction increasing up the ladder.



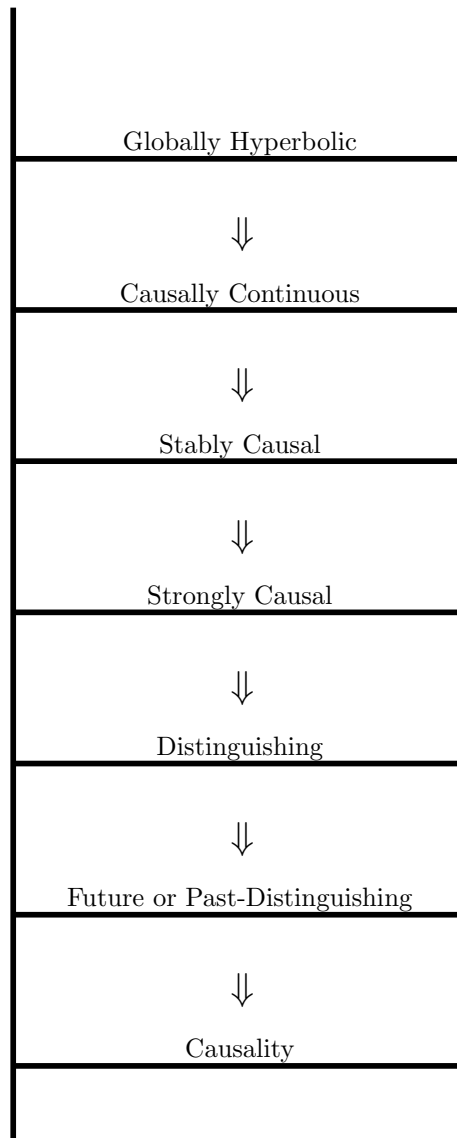


Figure 2.2: A ladder containing seven of the causal rungs which will be of interest in this paper. There are many more rungs not included here, however the ones in this schematic will be the only ones needed for our purposes. The rungs start with the least restrictive at the bottom, and ascend in order of increasing strictness of the causal condition. If a spacetime's causal structure satisfies a particular rung, then it satisfies all rungs below it, hence the implication arrows going down the ladder.

We now give definitions for the rungs on this causal ladder.

**Definition 34.** *A spacetime is causal if it contains no closed non-spacelike curves.*

**Definition 35.** *A spacetime is future-distinguishing if the chronological futures of any two points inside the spacetime are distinct sets. Similarly, a spacetime is past-distinguishing if the chronological pasts of any two points inside the spacetime are distinct sets.*

**Definition 36.** *A spacetime is said to be distinguishing if it is both past and future-distinguishing.*

**Definition 37.** *A spacetime is strongly causal if for any point  $p$  in the manifold, every neighborhood of  $p$  contains a sub-neighborhood which no causal curve intersects more than once. This definition can be rephrased in terms of causally convex neighborhoods by requiring that  $p$  has arbitrarily small causally convex neighborhoods in order for  $\mathcal{M}$  to be strongly causal at  $p$ .*

For the next rung of the causal hierarchy, we need to define the set of point-wise conformal metrics defined on a spacetime  $(\mathcal{M}, g)$ .

$$\text{Con}(\mathcal{M}) = \{\tilde{g} \mid \tilde{g}(x) = \Omega^2(x)g(x) \quad \forall x \in \mathcal{M}\}.$$

**Definition 38.** *A spacetime  $(\mathcal{M}, g)$  is stably causal if there exists  $\tilde{g} \in \text{Con}(\mathcal{M})$  such that  $g < \tilde{g}$  and  $\tilde{g}$  is causal.*

We can heuristically understand stable causality as being the condition that opening up the lightcones by an arbitrarily small amount does not allow for the appearance of closed causal loops in the spacetime.

**Definition 39.** *A spacetime is causally continuous if the set-valued maps  $I^{+/-}(p)$  are injective and continuous.*

**Definition 40.** *A spacetime is globally hyperbolic if it is strongly causal and  $\forall p, q, \in \mathcal{M}$ , sets of the form  $J^+(p) \cap J^-(q)$  are compact.*

### 2.3.1 Alternative Characterizations of Two Rungs

The definition of distinguishing given and used above uses chronological future and past. We can also give an equivalent definition, due to Minguzzi, which uses the causal future and pasts of points in the spacetime.

**Proposition 2.3.1.** *[9] Let  $\mathcal{M}$  be a spacetime containing points  $x, z$ . Then  $\mathcal{M}$  is distinguishing if and only if for every  $(x, z) \in J^+$ ,  $x \in J^+(z)$  implies  $x = z$ , and for every  $(a, b) \in J^+$ ,  $a \in \overline{J^-(b)}$  implies  $a = b$ .*

*Proof.* We will prove the future-distinguishing case, with the past-distinguishing case being completely analogous. We prove both implications by proving their contrapositives.

Consider the forward implication. Let  $x \neq z$  with  $(x, z) \in J^+$ , and  $x \in \overline{J^+(z)}$ . Then since  $(x, z) \in J^+ \iff z \in J^+(x)$ , we have  $I^+(z) \subset I^+(x)$ . On the other hand, since  $x \in \overline{J^+(z)}$ , we also have  $I^+(x) \subset I^+(z)$ , so  $I^+(x) = I^+(z)$ , and  $\mathcal{M}$  is not future-distinguishing.

Now for the reverse implication. If  $\mathcal{M}$  is not future-distinguishing, then there exists  $x' \neq z$  such that  $I^+(x') = I^+(z)$ . Note that  $z \in \overline{I^+(z)} = \overline{J^+(x')}$ . Now let  $\{z_n\}_{n \in \mathbb{N}}$  be a sequence of points in  $\mathcal{M}$  which converge to  $z$ . Let  $\{\sigma_n\}_{n \in \mathbb{N}}$  be a sequence of causal curves with past endpoint  $x'$  and future endpoint  $z_n$ , with  $\sigma$  being the limiting curve which passes through  $z$ . Then we can choose  $x \in \sigma$  where  $x \neq z$ . Then  $(x, z) \in J^+$  and  $x \in \overline{J^+(x')} = \overline{J^+(z)}$ , and the implication is proven.  $\square$

To more fully flesh out the important rung of strong causality, we give a proof of another equivalent condition for a spacetime to occupy the strongly causal rung of the causal ladder. We start with two lemmas, presented without proof as their results will be made use of in the proposition which immediately follows and are otherwise not of central focus to our aims.

**Lemma 2.3.2.** [10] *Let  $Q$  be an open set contained in a simple region,  $N$ , with a point  $p \in Q$ . Then there exist points  $u, v \in Q$  such that  $p \in \langle u, v \rangle_N \subset Q$ .*

The notation  $\langle u, v \rangle_N$  denotes the set of points,  $z \in N$  where  $z$  lies on a future-directed chronological curve which starts at  $u$  and ends at  $v$ , and is contained in  $N$ .

**Lemma 2.3.3.** [10] *Let  $N$  be a simple region containing points  $x$  and  $y$ . Then no future-directed causal curve lying in  $N$  can intersect  $\langle x, y \rangle_N$  in a disconnected set.*

**Proposition 2.3.4.** [10]  *$\mathcal{M}$  is strongly causal at  $p$  if and only if  $p$  is contained in a local causality neighborhood.*

*Proof.* We start with the forward implication. If  $\mathcal{M}$  is strongly causal at  $p$ , then we can place  $p$  in a simple region,  $N$ . We can furthermore find an open set  $Q \ni p$ , such that  $\overline{Q} \subset N$ . Since  $\mathcal{M}$  is strongly causal at  $p$ , we can find a causally convex neighborhood,  $L$  which contains  $p$ , and since  $L$  must be of arbitrary size, we ask that  $L$  is contained in  $Q$  making  $L$  a local causality neighborhood.

To prove the converse statement, suppose that  $p$  is contained in a local causality neighborhood,  $L$ , where  $L$  is contained in a simple region  $N$ . By Lemma 5.1, there exist points  $u, v \in L$  such that  $\langle u, v \rangle_N \subset L$ . Now let  $\gamma$  be a future-directed timelike curve which passes through  $\langle u, v \rangle_N$ . If  $\gamma$  intersects  $\langle u, v \rangle_N$  in a disconnected set, then by Lemma 5.2,  $\gamma$  is not fully contained in  $N$  and in fact intersects  $L$  in a disconnected set. But this contradicts the causal convexity of  $L$  (which was required for  $L$  to be a local causality neighborhood). Thus  $\langle u, v \rangle_N$  is causally convex, which means that  $\mathcal{M}$  is strongly causal at  $p$ .  $\square$

## Chapter 3

# Undergirdings for the Relationship between Causality and the Structure of Spacetime

The work of Robb, Zeeman, Kroheimer and Penrose, and others point toward a connection between causality, geometry, and topology. These three areas of inquiry give complementary descriptions of the structure of spacetime. Causal Set Theory furthermore posits a fundamental connection between causality and geometry. Let us trace some of the important results which motivate such a connection.

### 3.1 Causality and Conformal Geometry

We begin with a working following Hawking and Ellis which demonstrates how the physical notion of causal information determines conformal geometry [12]. This example will still reside in a continuous manifold setting. The ideological point being made is that one can use causal structure as the starting point of analysis, and arrive at a general geometric structure as a consequence. [12]

Begin with a normal neighborhood  $U$  in a 4-dimensional spacetime  $\mathcal{M}$ , where  $U$  contains the point  $p$ . Assign normal coordinates,  $\{x^\mu\}$  to  $U$ .

If one were given the set of points which can communicate with  $p$ , these would be the points reachable by a future-directed curve whose tangent vector never reaches a speed greater than the speed of light. These curves can be described by having coordinates which satisfy

$$-(x^0)^2 + (x^1)^2 + (x^2)^2 + (x^3)^2 \leq 0.$$

We can call this set  $C$  as follows

$$C \equiv \{x^\mu \in U \mid -(x^0)^2 + (x^1)^2 + (x^2)^2 + (x^3)^2 \leq 0\}.$$

Then the image of the set  $C$  under the exponential map forms the null cone around  $p$ ,  $N_p$  which is contained in  $T_p\mathcal{M}$ . Once the null cone through  $p$  is determined, we can determine the metric up to a conformal factor. We proceed as follows.

Let  $X \in T_p\mathcal{M}$  be timelike and  $Y \in T_p\mathcal{M}$  be spacelike. Then the bilinearity required of any generic metric,  $g_{\mu\nu}$  implies that the quadratic function

$$\begin{aligned} g_{\mu\nu}(X + \lambda Y)^\mu(X + \lambda Y)^\nu &= g_{\mu\nu}X^\mu X^\nu + 2\lambda g_{\mu\nu}X^\mu Y^\nu + \lambda^2 g_{\mu\nu}Y^\mu Y^\nu \\ &= a\lambda^2 + b\lambda - c \end{aligned}$$

has two real roots, since  $a = g_{\mu\nu}Y^\mu Y^\nu$  and  $c = -g_{\mu\nu}X^\mu X^\nu$  are both positive.

Now, if the null cone at  $p$ ,  $N_p$ , is known, then the roots of the above quadratic equation can be found. Since we do assume to have full knowledge of local causality in this example, we can find the roots and call them  $\lambda_1$  and  $\lambda_2$ .

By simply multiplying the quadratic formula expression for the two roots, we obtain the ratio

$$\lambda_1\lambda_2 = \frac{g_{\mu\nu}X^\mu X^\nu}{g_{\mu\nu}Y^\mu Y^\nu},$$

allowing us to compare the norms of a timelike and spacelike vector with each other.

Now we seek to compare any two non-null vectors with  $g_{\mu\nu}X^\mu X^\nu$ , so as to obtain the value of the metric on any two vectors up to a conformal factor. To this end, let  $W$  and  $Z$  be two non-null vectors. We assume  $W + Z$  is also non-null, for if it is not, we can simply substitute  $W + 2Z$  in the following working. We can write

$$g_{\mu\nu}W^\mu Z^\nu = \frac{1}{2}[g_{\mu\nu}W^\mu W^\nu + g_{\mu\nu}Z^\mu Z^\nu - g_{\mu\nu}(W + Z)^\mu(W + Z)^\nu]$$

Since  $W$ ,  $Z$ , and  $W + Z$  are non-null, we can compare each of the three values on the right hand side of the above equation with either the value of  $g_{\mu\nu}X^\mu X^\nu$  or  $g_{\mu\nu}Y^\mu Y^\nu$ , depending on whether  $W$ ,  $Z$ , and  $W + Z$  are themselves timelike or spacelike. Let us assume we compare with  $g_{\mu\nu}X^\mu X^\nu$  so as to compute

$$\frac{g_{\mu\nu}W^\mu Z^\nu}{g_{\mu\nu}X^\mu X^\nu}.$$

We have thus measured the metric up to a conformal factor based solely on local causality around the point  $p$ .

This working by Hawking and Ellis represents a critical logical inversion on the defining properties of spacetime in the following sense. Causality usually requires having the metric in hand in order to define the causal relations between

various spacetime events. It is with the capability to measure distances of spacetime intervals whereby one event can be deemed to influence another. In this logical fashion, the causal structure of spacetime is a derivative construction. Causal relations are built up from the output of the metric evaluated on two vectors in the tangent space, which requires one to know the metric beforehand.

By inverting the logic, however, one can derive nearly the full metric from only causal information. Hawking and Ellis demonstrate that local causal information is enough to measure the distances between any two vectors up to a conformal factor. Of course this distance measurement between any two vectors is tantamount to constructing the metric on the spacetime.

## 3.2 Causality and Topology

Topologies in general give us a way of describing the global structure of a space. In Causal Set Theory, it will be important to examine how a topological description of a space can be generated from manifold properties as well as by causal structure, and when these descriptions agree. This will help us develop intuition for the strongly causal rung of the causal ladder as well as provide the definition for a topology necessary for Johan Noldus' work on Lorentzian isometries.

We first require some basic topological definitions.

### 3.2.1 Topological Basics

**Definition 41.** *Given a set  $X$ , a topology on  $X$  is a set  $\mathcal{T}$  of subsets of  $X$ , whose elements are called open and satisfy the following:*

1.  $\emptyset \in \mathcal{T}, X \in \mathcal{T}$
2.  $\{\mathcal{U}_\alpha\}_{\alpha=1}^k \in \mathcal{T} \Rightarrow \bigcap_{\alpha=1}^k \mathcal{U}_\alpha \in \mathcal{T}$   
( $\mathcal{T}$  is closed under finite intersections)
3.  $\{\mathcal{U}_\alpha\}_{\alpha \in \mathbb{N}} \in \mathcal{T} \Rightarrow \bigcup_{\alpha \in \mathbb{N}} \mathcal{U}_\alpha \in \mathcal{T}$   
( $\mathcal{T}$  is closed under countable unions).

The double,  $(X, \mathcal{T})$  is a topological space.

**Definition 42.** *A family of open sets  $\{\mathcal{B}_\alpha\}_{\alpha \in \mathbb{N}}$  is a topological basis on a set  $X$  if:*

1. *Every element of  $X$  is contained in a basis element. That is,  $\forall x \in X, \exists B_x \in \{\mathcal{B}_\alpha\}_{\alpha \in \mathbb{N}}$  such that  $x \in B_x$*
2. *If an element of  $X$  belongs to the intersection of two basis elements, then there is a third basis element which contains  $x$  and is also contained in this intersection. That is,  $x \in B_1 \cap B_2 \Rightarrow \exists B_3 \in \{\mathcal{B}_\alpha\}_{\alpha \in \mathbb{N}}$  such that  $x \in B_3 \subset B_1 \cap B_2$*

**Definition 43.** A topological space,  $(X, \mathcal{T})$  is called Hausdorff, if  $\forall x, y \in X$  where  $x \neq y$ ,  $\exists U, V \in \mathcal{T}$  such that  $x \in U$  and  $y \in V$  and  $U \cap V = \emptyset$ . That is to say that any two distinct points can be separated by disjoint open sets.

We are also supplied with a useful definition of continuity.

**Definition 44.** A map between topological spaces,

$$f : (X_1, \mathcal{T}_1) \rightarrow (X_2, \mathcal{T}_2)$$

is continuous if and only if, for every open set  $V \in X_2$ ,  $f^{-1}(V)$  is open in  $X_1$ .

**Definition 45.** A map  $f$  is a homeomorphism if  $f$  is continuous and invertible with a continuous inverse.

**Definition 46.** A map  $f$  between open sets is a diffeomorphism if  $f$  is invertible and both  $f$  and  $f^{-1}$  are  $C^\infty$ .

**Definition 47.** A map  $f$  is an isometry if  $f$  is a diffeomorphism and  $f$  preserves the metric. That is,

$$f : (\mathcal{M}, g) \rightarrow (\mathcal{M}', g')$$

and  $g = f^*g'$  where  $f^*$  denotes the pullback of  $f$ .

**Definition 48.** A topological space,  $(X, \mathcal{T})$  is called second-countable if it has a countable basis. That is to say, there exists a countable family of open sets,  $\{\mathcal{U}_\alpha\}_{\alpha \in \mathbb{N}}$  such that any open set  $U \in \mathcal{T}$  can be formed by an indexed subset of this family,  $U = \bigcup_I \mathcal{U}_I$  for some index set  $I \subset \mathbb{N}$ .

Now let us see how general manifolds (defined earlier) can be endowed with a topology.

**Definition 49.** A topological manifold in  $d$ -dimensions is a Hausdorff, second-countable topological space, for which every point is contained in an open neighborhood which is homeomorphic to an open neighborhood in  $\mathbb{R}^d$ .

Recalling the definition of a manifold, we note that being a topological manifold is equivalent to requiring that open sets of  $\mathcal{M}$  can be formed as countable unions of the sets  $\{\mathcal{U}_\alpha\}_{\alpha \in \mathbb{N}}$  belonging to the atlas,  $\{\mathcal{U}_\alpha, \phi_\alpha\}_{\alpha \in \mathbb{N}}$ . This in turn makes each map  $\{\phi_\alpha\}_{\alpha \in \mathbb{N}}$  a homeomorphism.

Given a spacetime  $\mathcal{M}$ , we turn to describing a topology derived from the causal structure on  $\mathcal{M}$ .

### 3.2.2 Causal Topology and a New Characterization of Strong Causality

The culminating theorem of this section represents a second important inversion wherein topological structure is derived from causal information, rather than the other way around.

The first step towards the result is to construct a family of open sets using the causal information associated to points in the spacetime. The sets in question will be formed using the chronological pasts and futures of points in the spacetime, and are called Alexandrov intervals.

**Claim 2.** [10] *Sets of the form  $I^+(x) \cap I^-(y)$  where  $x, y \in \mathcal{M}$  form a topological basis on  $\mathcal{M}$ , for any causal spacetime  $\mathcal{M}$ .*

This topology is called the Alexandrov topology, denoted  $\mathcal{A}$ .

*Proof.* We first note that elements of  $\mathcal{A}$  are open by claim 1, since they are finite intersections of open sets. Now for  $\mathcal{A} := \{I^+(x) \cap I^-(y) | x, y \in \mathcal{M}\}$  to be a topological basis,  $\mathcal{A}$  must satisfy the two requirements of Definition 42.

1. To show aspect (1), we note that we can construct a timelike curve,  $\gamma(\lambda)$  through any point  $p \in \mathcal{M}$ . Then pick two points  $x, y \in \gamma(\lambda)$  such that  $x \ll p \ll y$ . Then by this construction,  $p \in I^+(x) \cap I^-(y)$ .
2. To show that if there are two elements  $A_1 = I^+(p) \cap I^-(q), A_2 = I^+(r) \cap I^-(s); A_1, A_2 \in \mathcal{A}$  such that  $x \in A_1 \cap A_2$ , then there is a third element,  $A_3 \in \mathcal{A}$  such that  $x \in A_3 \subseteq A_1 \cap A_2$ , we proceed as follows.

Suppose  $x \in [I^+(p) \cap I^-(q)] \cap [I^+(r) \cap I^-(s)]$ . Then  $x \in I^-(q) \cap I^-(s)$ , which is an open set since  $I^-(q)$  and  $I^-(s)$  are both open. This means there must exist another point  $u \in \mathcal{M}$  such that  $v \in I^-(q) \cap I^-(s)$  and we can demand that  $v$  lies just to the future of  $x$  by constructing a timelike path through  $x$  that has  $v$  as a future endpoint. So  $x \in I^-(v) \subseteq I^-(q) \cap I^-(s)$ .

By time-reversing the above logic, if  $x$  is an element of the open set  $I^+(p) \cap I^+(r)$ , then there exists  $u \in I^+(p) \cap I^+(r)$ . By drawing a timelike curve through  $x$  which is contained in  $I^+(p) \cap I^+(r)$ , we can ensure that  $x$  lies to the future of  $u$ . So  $x \in I^+(u) \subseteq I^+(p) \cap I^+(r)$ .

Hence  $x \in [I^+(u) \cap I^-(v)] \subseteq [I^+(p) \cap I^-(q)] \cap [I^+(r) \cap I^-(s)]$ .

□

The family of Alexandrov sets  $\mathcal{A} = \{I^+(x) \cap I^-(y) | x, y \in \mathcal{M}\}$  is indeed a topology on the spacetime  $\mathcal{M}$ . This topology has been constructed using only the causal structure on  $\mathcal{M}$ . While we have been loosely referring to this topology as coming from the causal structure on the spacetime, it is specifically built using the chronological structure, since the sets  $I^{+/-}$  were used. Penrose and Kronheimer, however, demonstrate that the horisomotic structure can be obtained from the causal structure [7]. Then, since as sets,  $I^+(p) = J^+(p) - E^+(p)$ , it is safe to say that we only need the causal structure to determine the Alexandrov topology.

Not only does a causal topology built using a basis of open chronological intervals exist, but under certain conditions, this topology is identical to the standard manifold topology of spacetime. The power of this result can be



contrasted with the previous derivation of the conformal metric using causal information, along the usual dividing line between geometry and topology.

The result of Hawking and Ellis functioned on a very local basis. They began by assuming knowledge of the causal information corresponding to a single point in spacetime (in particular, knowing the tangent space and null cone at that point). Proceeding from that information, the metric was built up by evaluating its output when given two vectors, and considering its value when fed two elements of the tangent space.

By contrast, the topology of a spacetime (or any manifold) is a global structure. The basis sets capture every element of the spacetime and allow for definitions of continuity and continuous maps defined on the entirety of the spacetime.

We now turn towards the conditions under which this causal topology  $\mathcal{A}$  is equivalent to the manifold topology.

To prepare for this important theorem, we require two important results.

**Lemma 3.2.1.** [10] *Let  $N$  be a simple region, containing an open set  $Q$ . Let  $p \in Q$ . Then there exist points  $u, v \in Q$  such that  $p \in [I^+(u) \cap I^-(v) \cap N] \subset Q$*

This first proposition is presented without proof as the reasoning involved is not key to the ultimate theorem or the larger question of this thesis. It will be used to help show that sets open in the manifold topology are open in the Alexandrov topology in theorem 3.2.3.

**Lemma 3.2.2.** [10] *Strong causality fails at  $p \in \mathcal{M}$  if and only if there exists  $q \in J^-(p)$ ,  $q \neq p$ , such that  $x \in I^-(p)$  and  $q \in I^-(y)$  together imply  $x \in I^-(y)$   $\forall x, y \in \mathcal{M}$ .*

*Proof.* As a form of proof, we present Figure 3.1 which depicts violation of strong causality at  $p$  according to the necessary equivalence condition mentioned in the lemma.

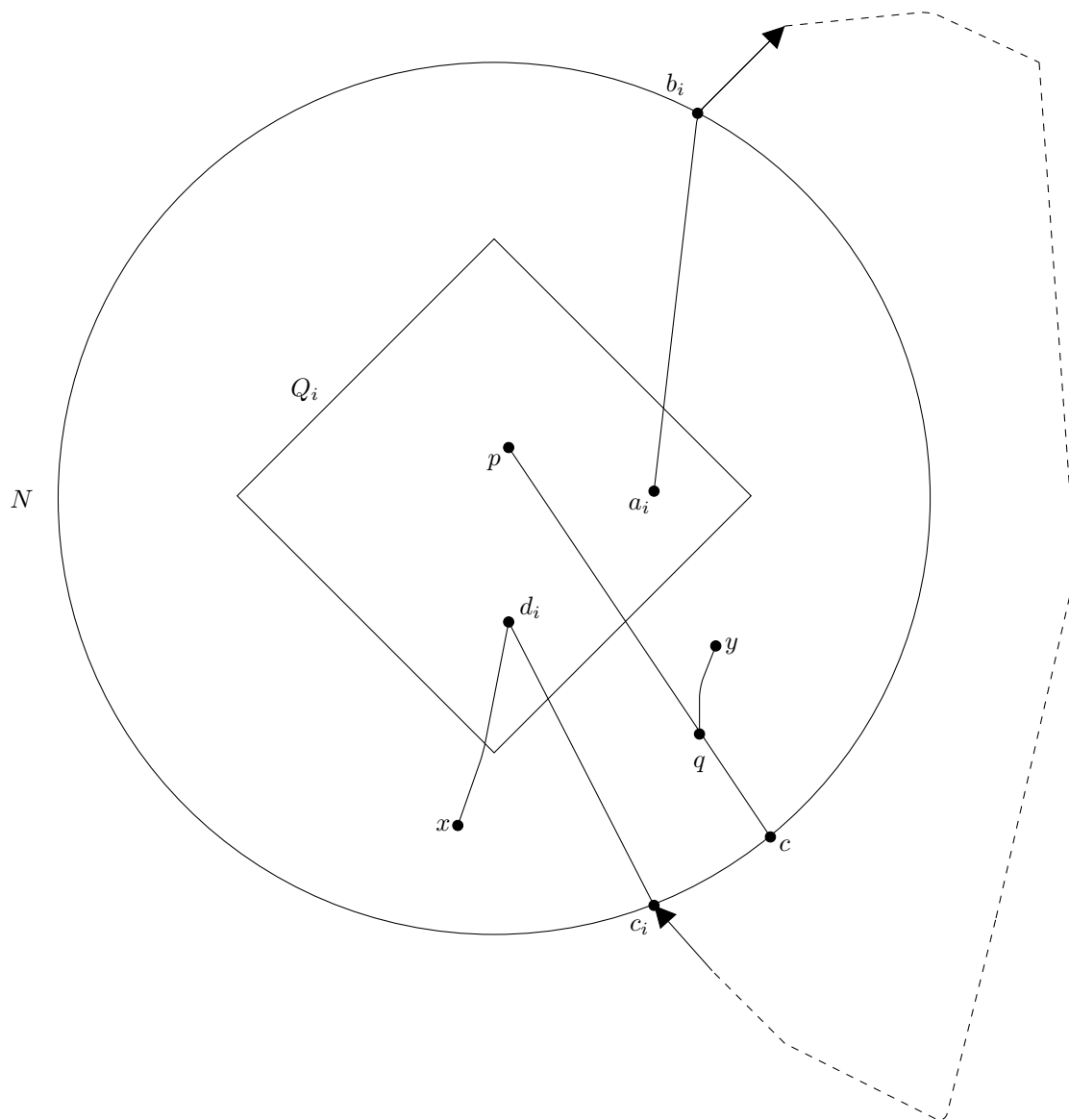


Figure 3.1: This image illustrates all of the required conditions and results (and the results reversed with the conditions to show the converse), of Lemma 3.2.2. Namely, we have a point  $p \neq q \in J^-(p)$ ,  $q \in I^-(y)$ , and  $x \in I^-(p)$ , and a curve,  $\gamma$  such that  $\gamma \cap N$  (where  $N$  is a simple region containing  $p$  not mentioned in the lemma) is future directed and timelike. The neighborhood  $Q_i := \langle u_i, v_i \rangle$ , as well as the entry and exit points of  $\gamma$  from  $N$  carry indices since it is important that such a diagrammatic reality hold for *any* neighborhood  $Q_i$  containing  $p$  in order for strong causality to fail there.

□

**Theorem 3.2.3.** [10] *The following three conditions on a spacetime  $\mathcal{M}$  are equivalent:*

1.  $\mathcal{M}$  is strongly causal
2. the Alexandrov topology agrees with the manifold topology
3. the Alexandrov topology is Hausdorff

*Proof.* To show (1) implies (2), we must show that given strong causality on  $\mathcal{M}$ , sets open in the manifold topology are open in the Alexandrov topology, and sets open in the Alexandrov topology are open in the manifold topology. Suppose strong causality holds at a point  $p \in \mathcal{M}$ . Let  $P$  be an open set containing  $p$ , and let  $N \subset P$  be a simple region which also contains  $p$ . Since strong causality holds at  $p$ , we can also find a causally convex set,  $Q \subset N$  containing  $p$ . By Lemma 3.2.1, there must exist points  $u, v \in Q$  such that  $p \in (I^+(u) \cap I^-(v) \cap N) \subset Q$ . We now require that  $I^+(u) \cap I^-(v) \cap N = I^+(u) \cap I^-(v)$ . This must be, since if  $I^+(u) \cap I^-(v) \cap N \neq I^+(u) \cap I^-(v)$ , it would imply a timelike path between  $u$  and  $v$  which leaves and reenters  $N$ , and by implication,  $Q$  as well. This, however, would violate the causal convexity of  $Q$ . Thus  $I^+(u) \cap I^-(v) \cap N = I^+(u) \cap I^-(v)$ , and we have succeeded in placing a neighborhood which is open in the Alexandrov topology around  $p$ . So the sets open in  $\mathcal{T}_{\mathcal{M}}$  are open in  $\mathcal{A}$ . That sets open in  $\mathcal{A}$  are open in  $\mathcal{T}_{\mathcal{M}}$  is clear since the elements of  $\mathcal{A}$  consist of the intersection of two open (in  $\mathcal{T}_{\mathcal{M}}$ ) sets.

Seeing that (2) implies (3) is clear since  $\mathcal{T}_{\mathcal{M}}$  was assumed to be Hausdorff to start.

Now to show (3) implies (1). We proceed towards a contradiction by supposing that strong causality fails at  $p \in \mathcal{M}$ . Suppose  $q$  lies in the causal past of  $p$  and let  $p$  and  $q$  be contained in the Alexandrov sets,  $p \in I^+(x) \cap I^-(u)$ ,  $q \in I^+(v) \cap I^-(w)$ . We note that  $q$  being in the causal past of  $p$ , together with  $p$  being in the chronological past of  $u$  implies that  $q$  is in the chronological past of  $u$ . Further, we can choose a point  $y \in I^+(v) \cap I^-(w)$ , such that  $q$  lies in the chronological past of  $y$  and  $y$  is also an element of the chronological past of  $u$ . Now by Lemma 3.2.2,  $x$  lies in the chronological past of  $y$ , which means that  $y$  is an element of both  $I^+(x)$  and  $I^-(u)$ , ie  $y \in I^+(x) \cap I^-(u)$ . But now,  $y \in [I^+(x) \cap I^-(u)] \cap [I^+(v) \cap I^-(w)]$ , which means that the covering Alexandrov elements of two distinct points of  $\mathcal{M}$  have a nontrivial intersection, meaning the Alexandrov topology fails to be Hausdorff. Thus,  $\mathcal{A}$  being Hausdorff implies that  $\mathcal{M}$  is strongly causal.

□

So as long as our manifold occupies the strongly causal rung of the causal ladder, and the standard topology is Hausdorff, the Alexandrov topology is the same as the manifold's inherent topology. Given one has a strongly causal spacetime then, having access to the global causal structure of the spacetime is equivalent to knowing the topology of the spacetime.

It is interesting to note that the causal condition required to access the global topological structure is that of strong causality. Strong causality as a condition has a peculiar sort of global nature, even when defined at a single point. Strong causality at a single point  $p \in \mathcal{M}$  requires that one be able to place a neighborhood of arbitrary size around  $p$  such that no future directed causal curve ever intersects this neighborhood twice. Asking that no future directed causal curve behave in this way, however, does not concern the behavior of the curve only in the (arbitrarily small) neighborhood of  $p$ , but requires that the curve never comes back to a specified region of the spacetime. This is a demand on the behavior of the curve everywhere on its codomain, which could intersect arbitrarily large portions of the spacetime.

However, the payoff is considerable. If one is given the causal structure on a spacetime which occupies the strongly causal rung of the causal ladder, then one knows the complete topological structure of the spacetime.

## Chapter 4

# Building up to the Central Conjecture of Causal Set Theory

S.W. Hawking, A.R. King, and P.J. McCarthy’s 1976 work is when we begin to take notice of the specific rung of the causal ladder where results function. By following Zeeman’s work and moving from an automorphism on a particular spacetime to a bijection between two spacetimes, Hawking, King and McCarthy arrived at a relation between *different* spacetimes based on a chronology preserving map.

### 4.1 Three Key Theorems of Hawking

We first define the map in question.

**Definition 50.** *Let  $\mathcal{M}_1$  and  $\mathcal{M}_2$  be two spacetimes, with chronology relations  $\ll_1$  and  $\ll_2$  respectively. Then a map  $f : \mathcal{M}_1 \rightarrow \mathcal{M}_2$  is a chronological bijection if  $f$  is a bijection and,  $\forall x, y \in \mathcal{M}_1$ ,*

$$x \ll_1 y \iff f(x) \ll_2 f(y).$$

Given this definition, we can state the main result of Hawking, King and McCarthy.

**Theorem 4.1.1.** *[13] If a chronological bijection exists between two strongly causal spacetimes of dimension  $d > 2$ , then these spacetimes are conformally isometric.*

In fact, theorem 4.1.1 did not appear this way in the original paper by Hawking, King and McCarthy. Their paper, [13], dealt with a new topology on spacetime, which they called the “path topology,” denoted  $\mathcal{P}$ , on which

homeomorphisms could be defined which in turn encoded parts of the geometric, topological and causal structure of spacetime.

A function  $f$  that is a homeomorphism with respect to  $\mathcal{P}$  has many useful properties. Such an  $f$  is also a homeomorphism with respect to the Alexandrov topology, and in the presence of strong causality,  $f$  is a homeomorphism with respect to the manifold topology. In the presence of strong causality, a  $\mathcal{P}$ -homeomorphism also either preserves or reverses both causal and chronological relations and preserves null geodesics. The group of  $\mathcal{P}$ -homeomorphisms on a spacetime is ultimately shown to be the same as the group of conformal diffeomorphisms. Theorem 4.1.1 works when the dimension is greater than 2, and the map in question preserves (never reverses) chronological relations.

While theorem 4.1.1 generalized Zeeman's work by trading an automorphism for a bijection between different manifolds, we note that the new result holds only for the rather restrictive condition of strong causality. Subsequent work by David Malament generalized Theorem 4.1.1 by lowering the rung on the causal ladder where the result of conformal isometry is valid. The rung was lowered to distinguishing. The following is referred to as the Hawking-King-McCarthy-Malament (HKMM) Theorem.

**Theorem 4.1.2.** *[14] If a chronological bijection exists between two future and past-distinguishing spacetimes of dimension  $d > 2$ , then these spacetimes are conformally isometric.*

Work by Kronheimer and Penrose showed that chronological bijections are implied by causal bijections [7]. Further work by Parikar and Surya showed that the assumptions of Theorem 1.2 above are sufficient to determine the dimension of the spacetimes in question [15]. This allowed for the extension of the HKMM theorem to the following.

**Theorem 4.1.3.** *[15] If a causal bijection exists between two future and past-distinguishing spacetimes,  $\mathcal{M}_1$  and  $\mathcal{M}_2$ , with dimensions  $d_1$  and  $d_2$  respectively, then  $\mathcal{M}_1$  is conformally isometric to  $\mathcal{M}_2$ , and the spacetimes have the same dimension, that is  $d_1 = d_2$ .*

This result, which channels decades of analysis of the causal structure of spacetime into geometric revelations does so to a remarkable level. We can safely say now, that the causal structure of spacetime is equivalent to the conformal geometry of spacetime.

Conformal geometry, however, is not the full geometry of a manifold. In  $d = 4$  dimensions, there are in general 10 degrees of freedom to the metric tensor. The causal structure gives us everything but the conformal factor, which can be captured in the local volume element. As David Finkelstein tells us, the causal structure in  $d = 4$  is 9/10 of the metric [16].

We can decompose the two elements necessary for recovering the geometry of spacetime according to the slogan

$$\text{Order} + \text{Volume} = \text{Lorentzian Geometry.}$$

And it is in this crucial 1/10 of information where Causal Set Theory posits discreteness to play a role. To make contact with the metric's volume element and the final piece of information to access the full Lorentzian geometry of spacetime, we substitute a finite number of spacetime elements.

The aim of Causal Set Theory may be framed as leveraging the notions of order and causality, which exist at a kinematic level, before ever coming to quantum probabilities, in order to fully characterize the geometry of spacetime [17]. The existence at a kinematic level is important here, and marks a departure from typical quantum theories of other observables. In the case of Causal Set Theory, spacetime is indeed a causal set, and the continuous manifold description of spacetime is merely an approximation to the underlying causal set.

We are further motivated to think of continuum spacetime as an approximation to the underlying discrete causal set because causality in the continuum does not provide enough information to measure the full metric of the spacetime. As Hawking's theorem demonstrated, two spacetimes with the typical differentiable structures which can be bijectively mapped into each other without losing causal information can only be deemed *conformally* isometric.

The continuum does not furnish a way to measure the volume element, or the missing 1/10th of the metric. By appealing to the discrete description of spacetime, however, the volume of a region of spacetime can be supplanted with *counting*. Specifically, a count of the number of causal set-elements which lie in a specified region of spacetime. Such a counting process requires only the identification of elements in spacetime, and an at most countably-infinite number. Such a count requires no more structure or knowledge of the spacetime, and supplies us with the last vital piece of information to describe the full metric of spacetime and access its full suite of geometric features.

Riemann would have called this underlying set of spacetime events a "discrete ordered manifold" – a set with a particular order relation and a discrete number of points. We will call it a causal set.

**Definition 51.** *The double  $(C, <)$ , is a causal set if the following conditions hold.*

1.  $<$  is a reflexive partial order on  $C$
2.  $\forall a, b \in C, |Future(a) \cap Past(b)| \in \mathbb{N}$

Condition (2) is interpreted as the requirement that the number of spacetime elements in any *order interval* is finite. An order interval is here composed of all the points in the future of point  $a$  which can be influenced by  $a$ , and the past of  $b$  being all the points which lie in  $b$ 's past which could have communicated with  $b$ .

The definition of an abstract causal set motivates the discrete version of the slogan stated above, where volume is replaced by number.

$$Order + Number = Lorentzian \ Geometry.$$

Discreteness must be situated in the manifold in such a way as to be compatible with its continuous structure. This compatibility is achieved through faithful embeddings, which play crucially into the central conjecture, or *hauptvermutung* of Causal Set Theory.

## 4.2 The *Hauptvermutung* of Causal Set Theory

We start by giving the definition of a faithful embedding.

**Definition 52.** *A faithful embedding,  $f$ , is an injection from the causal set to the spacetime  $\mathcal{M}$  such that:*

1. *The number-volume correspondence is satisfied: for any subset  $O$  of  $M$ , the number of causal set elements in  $O$  is roughly equal to the (sprinkling density multiplied by the) volume of  $O$ .*
2.  *$f$  is order preserving.*

The number-volume correspondence requires that the discrete notion of number or set cardinality (an integer-valued quantity), be roughly preserved in its continuum incarnation as volume. Condition (2) requires that the causal order of the discrete and the continuous spacetimes be compatible.

We need a process for constructing a faithful embedding that will not only satisfy these relations between the discrete and continuum, but will also satisfy Lorentz symmetry in a way that previous attempts at discretization were not able to. What we seek is a Poisson sprinkling, which will be defined in the next chapter.

Equipped with the definition of a causal set, we can state the central conjecture, or *hauptvermutung* of Causal Set Theory. The *hauptvermutung* of Causal Set Theory assesses the circumstances under which continuum spacetimes are reasonable approximations to discrete causal sets.

The statement of the *hauptvermutung* varies across sources, while its core contents remain the same. In the foundational 1987 paper by Bombelli, Lee, Meyer, and Sorkin, the *hauptvermutung* is framed not as a formal conjecture to be proven, but as a sensible conclusion one should be able to draw based on the correspondence between faithfully embedded causal sets and their manifold approximations [18]. In this paper, Bombelli et. al state that if there exists a manifold,  $(\mathcal{M}, g)$  in which a causal set  $C$  can be faithfully embedded, then

“[Their] discussion leads [them] to expect that it is essentially unique. In other words, [they] can expect that any pair of faithful embeddings,  $f_1 : C \rightarrow (\mathcal{M}_1, g_1)$  and  $f_2 : C \rightarrow (\mathcal{M}_2, g_2)$  are related by a  $C$ -preserving diffeomorphism,  $h : \mathcal{M}_1 \rightarrow \mathcal{M}_2$  which is an approximate isometry of  $g_1$  to  $g_2$ .”

A 2018 review by Sumati Surya formalizes this to an extent as follows [17].

**Conjecture 1.** *A causal set  $C$  can be faithfully embedded at density  $\rho_C$  into two distinct spacetimes  $(\mathcal{M}, g)$  and  $(\mathcal{M}', g')$  if and only if the spacetimes are approximately isometric.*



Surya elaborates on the statement of the *hauptvermutung* in a way that will hint at the use of moduli spaces of Lorentzian manifolds as follows. Let us denote the set of all possible Lorentzian manifolds by  $\mathcal{L}$ . Let  $\sim$  denote approximate isometry at a density  $\rho_C$  between elements of  $\mathcal{L}$ . And let us denote by  $\Omega_C$  the set of all causal sets which have manifold approximations (these approximations being manifolds in  $\mathcal{L}$ ). Then there is a correspondence between the quotient space,  $\mathcal{L} / \sim$  and  $\Omega_C$ . These three statements of the *hauptvermutung* will be discussed in more detail in chapter 8.

The aim of this thesis will be to examine the following question:

For which rungs of the causal ladder does the *hauptvermutung* hold true? In reference to [18], our question is: given a spacetime with a faithfully embedded causal set, when is this spacetime unique? In particular, what rung of the causal ladder must the spacetime occupy in order to be unique? That is to ask, what causal restriction must a spacetime satisfy in order for a faithful embedding of a causal set to fully identify the spacetime up to approximate isometry?

The *hauptvermutung* contains some ill-defined notions which will require more precise formulations if one hopes to deliver an answer to our questions or a proof of the *hauptvermutung* itself. Perhaps the central vaguery is the notion of “essential uniqueness”. Even Surya’s more formal statement positing essential uniqueness to mean “approximate isometry” is not clearly defined. The issue of essential uniqueness and approximate isometry will be discussed in the final chapter of this paper with a possible definition and path forward presented.

## Chapter 5

# Obtaining Faithful Embeddings: Poisson Processes

A Poisson process is a way of picking a finite number of points from a spacetime at random, where the selection of one point is independent from all others. The number of points selected from a particular region of spacetime is on average, equal to the volume of the region, multiplied by the sprinkling density. Not only do these features help satisfy the first requirement of a faithful embedding, they ensure that a Poisson process does not pick out a preferred direction, and thus on average satisfies Lorentz invariance.

As a distribution of a discrete random variable, the Poisson distribution is the limit of a binomial distribution where the number of trials,  $n$  is taken to the infinity and the probability of success in each event,  $p$ , is taken to 0, while leaving the quantity  $np$  constant. Let us recall the binomial distribution and then observe the limiting behavior.

Consider a set of  $n$  independent events,  $\{A_i\}_{i=1}^n$ , each with a likelihood  $p$  of occurring. The number of events,  $k$ , that occur is a random variable,  $X$ , given by the binomial distribution,

$$\mathbb{P}(X = k) = \frac{n!}{k!(n-k)!} p^k (1-p)^{n-k}.$$

Now consider the behavior of this distribution where we define the parameter  $\lambda = np$  which is kept constant, and then take  $n \rightarrow \infty$ .

$$\begin{aligned}
\mathbb{P}(X = k) &= \frac{n!}{k!(n-k)!} p^k (1-p)^{n-k} \\
&= n(n-1)\dots(n-k+1) \frac{\left(\frac{\lambda}{n}\right)^k \left(1 - \frac{\lambda}{n}\right)^n}{k! \left(1 - \frac{\lambda}{n}\right)^k} \\
&= 1\left(1 - \frac{1}{n}\right)\dots\left(1 - \frac{k-1}{n}\right) \frac{\lambda^k \left(1 - \frac{\lambda}{n}\right)^n}{k! \left(1 - \frac{\lambda}{n}\right)^k}
\end{aligned}$$

Now note the following limits:

$$\begin{aligned}
\lim_{n \rightarrow \infty} \prod_{l=0}^{k-1} \left(1 - \frac{l}{n}\right) &= 1 \\
\lim_{n \rightarrow \infty} \left(1 - \frac{\lambda}{n}\right)^n &= e^{-\lambda} \\
\lim_{n \rightarrow \infty} \left(1 - \frac{\lambda}{n}\right)^k &= 1.
\end{aligned}$$

So we see that

$$\lim_{n \rightarrow \infty} \mathbb{P}(X = k) = \frac{\lambda^k e^{-\lambda}}{k!},$$

which is precisely the Poisson distribution with parameter  $\lambda$ .

In our setting, the random variable is the cardinality of the causal set abstracted from the spacetime. For this reason, we will often write  $\mathbb{P}(|X| = k)$  where  $X$  is interpreted as an at most countable set with cardinality  $|X|$  and we are measuring the probability that  $X$  consists of  $k$  elements.

In order to define a Poisson process, let us recall a few necessary definitions.

**Definition 53.** *A measure,  $\mu$ , is a non-negative and countably additive set function.*

In the setting of Causal Set Theory, the measure of interest will be the Lorentz volume measure. Given a metric tensor  $g_{\mu\nu}$  with determinant  $g$ , the Lorentz volume of a region  $U$  of our spacetime  $\mathcal{M}$  in  $d$ -dimensions is given by

$$\int_U \sqrt{-g} d^d x.$$

This measure calculates volume, which is of course dimensionful. The output of a Poisson process is the number of elements selected at random from a

region of spacetime, and as such must be dimensionless. The parameter  $\lambda$ , therefore, cannot be simply the area of a region of spacetime. We remedy this by introducing a density,  $\rho \sim \text{volume}^{-1}$ , associated to our Poisson process. From this we write the parameter our Poisson process as

$$\lambda = \rho * \text{Vol}(U),$$

where  $\text{Vol}(U) = \int_U \sqrt{-g} d^d x$ , and  $\lambda$  is now dimensionless. When we run Poisson processes on a region of spacetime,  $U$  is generally fixed.

**Definition 54.** *Given a spacetime  $\mathcal{M}$ , a Poisson process run on  $\mathcal{M}$  with density  $\rho$  is a random countable subset of  $\mathcal{M}$ , such that*

1. *For any family of random countable subsets,  $\{X_i\}_{i \in \mathbb{N}}$  of  $\mathcal{M}$ , the random variables  $\{|X_i|\}_{i \in \mathbb{N}}$  are independently distributed*
2. *The random variables  $\{|X_i|\}_{i \in \mathbb{N}}$  take values according to the Poisson distribution, that is,  $\forall i$  we have*

$$\mathbb{P}(|X_i| = k) = \frac{(\rho * \text{Vol}(\mathcal{M}))^k e^{-(\rho * \text{Vol}(\mathcal{M}))}}{k!}$$

Physically, we choose a volume parameter which corresponds to a minimal volume cutoff, above which we require our measurements to be accurate. Since we are after a theory of quantum gravity, the volume cutoff of interest will be derived from the Planck length:

$$l_P = \sqrt{\frac{\hbar G}{c^3}},$$

$$V = l_P^4.$$

Then  $\rho \sim l_P^{-4}$ . This choice of density sets the discreteness scale.

A Poisson process seems to satisfy a statistical version of Lorentz invariance, since each point in the resulting finite subset is picked uniformly at random, and independently of all others.

Does it also satisfy the number-volume correspondence required of faithful embeddings? That is, does the number of elements picked from a region of spacetime equal on average, the volume of that spacetime?

We must compute the expectation value of the Poisson distribution.

$$\begin{aligned}
\mathbb{E}(|X| = k) &= \sum_k k \mathbb{P}(|X| = k) \\
&= \sum_k k \frac{(\rho * Vol(\mathcal{M}))^k e^{-\rho * Vol(\mathcal{M})}}{k!} \\
&= \sum_k (\rho * Vol(\mathcal{M}))^k \frac{1}{(k-1)!} e^{-\rho * Vol(\mathcal{M})} \\
&= \sum_k (\rho * Vol(\mathcal{M})) \frac{(\rho * Vol(\mathcal{M}))^{k-1}}{(k-1)!} e^{-\rho * Vol(\mathcal{M})} \\
&= \sum_k (\rho * Vol(\mathcal{M})) \\
&= \rho * Vol(\mathcal{M}).
\end{aligned}$$

So the average value of the Poisson distribution is indeed the number of points selected from the region  $\mathcal{M}$ .

To see that condition (2) of a faithful embedding is realized, we need to proceed from the Poisson process to the notion of a *sprinkling* in which the Poisson process is subsumed. After a finite set of points from the spacetime manifold are selected through the Poisson process, sprinkling adds two properties to the selected points.

1. The selected points are endowed with the order inherited from the light cone structure on the spacetime. This gives rise to a causal set.
2. The points are abstracted from the spacetime, forgetting their manifold existence. They are now points in a random causal set of finite order.

With a sprinkling Poisson process, we see that condition (2) of a faithful embedding is achieved. From before, the number volume correspondence is satisfied since the number of elements in a causal set will be approximately the area of the spacetime, that is  $\mathbb{E}(|X| = k) = \rho * Vol(\mathcal{M})$ , and now the causal order is preserved by endowing points with their manifold causal relations.

To produce a faithful embedding, we typically select points already lying in the manifold  $M$  to constitute the causal set. In this way, a spacetime gives rise to a class of causal sets, with variable density.

## Chapter 6

# Analyzing Causal Peculiarities

In this chapter we build up intuition for certain different rungs of the causal ladder by examining spacetimes with specific causal peculiarities. All the example spacetimes in this section are flat and two dimensional.

We will explore three spacetimes. Each spacetime occupies a specific rung on the ladder, and manifestly does not belong to the rung directly above it, so that we can isolate the rung in question and observe it in detail.

In the following discussion, we use the convention that filled arrowheads denote future-directed curves, and empty arrowheads denote past-directed curves.

### 6.1 Past but Not Future-Distinguishing

Figure 6.1 below gives us an example of a flat two-dimensional spacetime which is past-distinguishing but not future-distinguishing [14]. In particular, the causal futures of all points on the line  $t = 0$  are all the same, and consist of the entire upper half of the spacetime. To see this, we need to analyze the metric which induces the tilting light cone structure, wherein the lightcones on the  $t = 0$  line lie at 90 degrees to the horizontal, while as  $|t| \rightarrow \infty$ , the null cones are at 45 degrees.

By examining Figure 6.1, one can see that we can reach any point to the upper left of point  $p$  by either moving in a straight line, or moving along the null  $t = 0$  line and then moving up along a causal line.

It is unclear, however, if we can reach points above the line  $t = 0$  and to the left of  $p$ .

Let us construct a causal curve which takes us from  $p$  at  $(x_1, 0)$  to  $(x_2, t_1)$ , which is arbitrarily close to  $p$ , so  $|x_2 - x_1| \ll 1$ , and  $t_1 \ll 1$ .

The line element for the spacetime is given as

$$\begin{aligned} ds^2 &= (\cosh(t) - 1)^2(dt^2 - dx^2) + dt dx \\ &= f(t)(dt^2 - dx^2) + dt dx. \end{aligned}$$

So we are able to write the metric as

$$g_{\mu\nu} = \begin{pmatrix} f(t) & \frac{1}{2} \\ \frac{1}{2} & -f(t) \end{pmatrix}.$$

To determine the signature of our metric we compute its determinant. Since  $\det(g_{\mu\nu}) = -[f(t)^2 - \frac{1}{4}]$  is negative, the metric  $g_{\mu\nu}$  has one positive and one negative eigenvalue.

Hence we work in  $(+, -)$  signature, meaning that a vector  $v$  is causal if  $v^2 \geq 0$ .

Let us parametrize a path  $\gamma$  by  $\lambda \in [0, 1]$  and set

$$\begin{aligned} t(\lambda) &= \lambda t_1 \\ x(\lambda) &= x_2 + \lambda(1 - x_2 + x_1), \end{aligned}$$

so that  $\gamma(\lambda) = (\lambda t_1, x_1 + \lambda(1 - x_2 + x_1))$  and  $\gamma'(\lambda) = (t_1, (1 - x_2 + x_1))$ .

Now we show that  $\gamma(\lambda)$  is a causal curve. For neatness, we rename  $1 - x_2 + x_1 =: a$ .

We compute

$$\begin{aligned} \gamma'(\lambda)^2 &= \gamma'(\lambda)^\mu \gamma'(\lambda)^\nu g_{\mu\nu} \\ &= (t_1, a) \begin{pmatrix} f(t) & \frac{1}{2} \\ \frac{1}{2} & -f(t) \end{pmatrix} \begin{pmatrix} t_1 \\ a \end{pmatrix} \\ &= t_1[f(t)t_1 + \frac{1}{2}a] + a[\frac{1}{2}t_1 - f(t)a] \\ &= at_1 + f(t)t_1^2 - f(t)a^2. \end{aligned}$$

Now insert the second-order expansion,  $\cosh(t) = 1 + \frac{t^2}{2!} + O(t^4)$  into  $f(t)$  in the neighborhood  $t \in [0, t_1]$ . Then, to this order,

$$f(t) = \frac{t^4}{4} = \frac{(\lambda t_1)^4}{4}.$$

Plugging this form of  $f(t)$  into the last line above gives

$$\gamma'(\lambda)^2 = at_1 + \frac{\lambda^4 t_1^6}{4} - \frac{\lambda^4 t_1^4}{4} a^2,$$

which, for  $t_1$  infinitesimally small, is dominated by the linear term in  $t_1$ . Hence  $\gamma'(\lambda)^2 \geq 0$ , and  $\gamma(\lambda)$  is causal curve.

This calculation, combined with the observation that any point to the upper right of  $p$  (or any other point on  $t = 0$ ) can be reached by a straight line – either emanating from the point on  $t = 0$  or by moving to the right along this line and then moving up along a causal line – demonstrates that the causal future of any point on the  $t = 0$  line consists of the entire upper half of the cylinder.



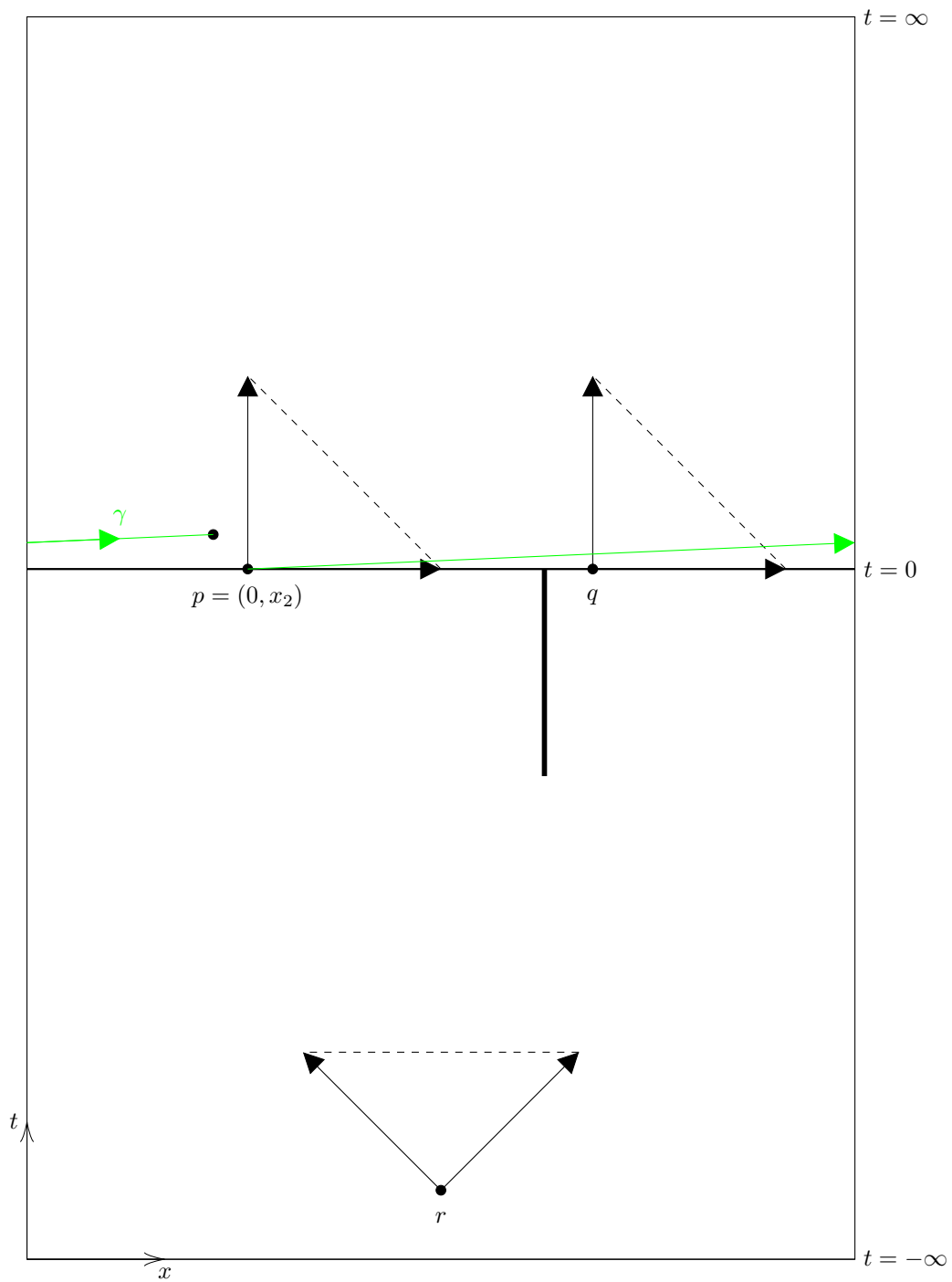


Figure 6.1: A spacetime given by an unfurled cylinder where the left and right edges have been identified. The spacetime is past-distinguishing, however it fails to be future-distinguishing at  $t = 0$ . The causal futures of all points along the line  $t = 0$  are identical and consist of the entire top half of the cylinder.

## 6.2 Distinguishing but Not Strongly Causal

Figures 6.2 and 6.3 below give an example of a spacetime which is distinguishing but which fails to be strongly causal [12]. The spacetime has two excisions, depicted with bold lines. The null line connecting the endpoints of these excisions is given by a dashed line.

In Figure 6.2, a point from each of the roughly 3 regions of the spacetime has been chosen with curves depicting that strong causality holds nearly everywhere on this spacetime. The goal in Figure 6.2 is to show that strong causality holds on most of the spacetime because a causal curve cannot come back to a neighborhood set up around a point in these regions.

A causal curve starting from a neighborhood around any point below the lower excision will run into one of the two excisions. Similarly a curve starting from a neighborhood around any point above the upper excision will run into one of the two excisions. We note that we use future or past-directed curves where they are convenient. If a past-directed curve cannot come back to the neighborhood in which it started, then neither can a future-directed curve.

A causal curve beginning from a neighborhood around a point in between the two excisions has the chance to initially evade the excisions, but will eventually run into one of the excisions as it tries to return to the neighborhood around its starting point. These restrictions are almost enough to ensure strong causality.

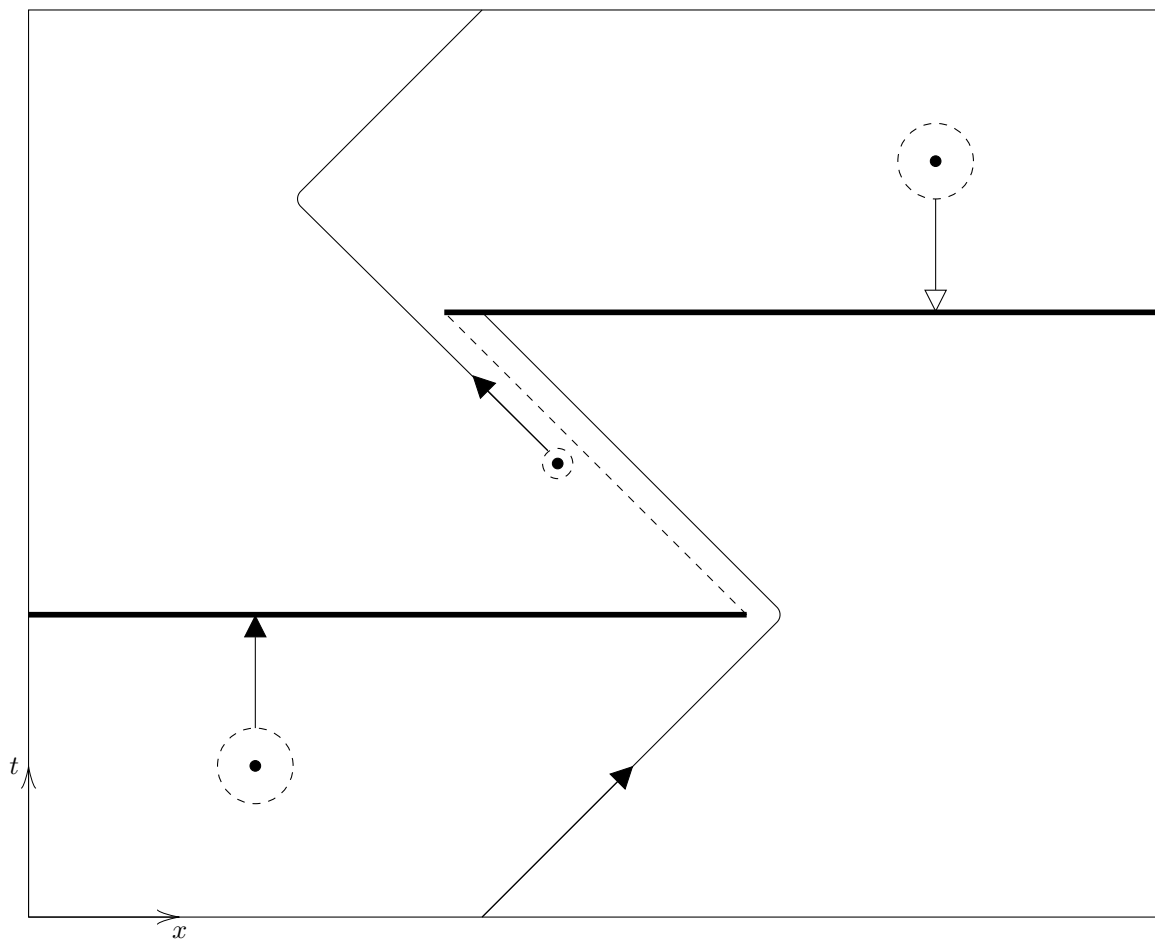


Figure 6.2: Another spacetime given by an unfurled cylinder, this time with the top and bottom edges identified. Two horizontal excisions (in bold) have been made. The spacetime is strongly causal almost everywhere. However, as we near the null geodesic connecting the excisions (given by the dotted line), we approach the problematic region of the spacetime.

Indeed, the only region of this flat two-dimensional spacetime where strong causality fails is on the null line connected the endpoints of the two excisions.

Strong causality fails at every point on the dashed line. As shown, around every point on this null line, a curve can be constructed which gets arbitrarily close to its starting point, meaning it will re-enter the neighborhood it came from and violate strong causality. Strong causality, even at a particular point, carries a peculiar global requirement. At any point in the manifold, a causal curves which intersect neighborhoods of the point in question must never return, as Figure 6.3 demonstrates.

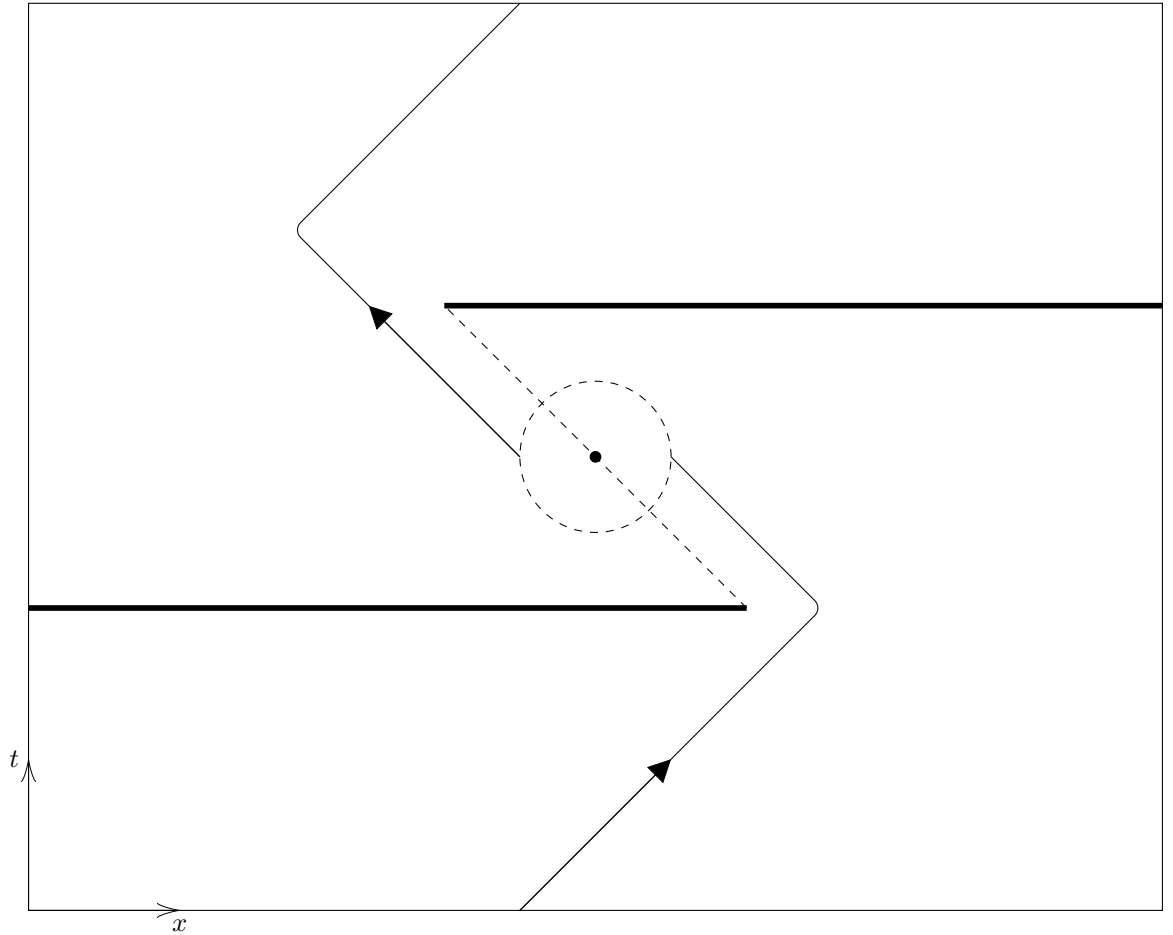


Figure 6.3: The dotted null geodesic is the region of this spacetime where strong causality fails. As we see, we can take a future directed causal curve and making use of the top-bottom identification, intersect any neighborhood of any point on this null geodesic twice.

### 6.3 Strongly Causal but Not Globally Hyperbolic

The next illustration in Figure 6.4 gives an example of a strongly causal spacetime which fails to be globally hyperbolic. Such a spacetime will also be used in the next chapter. Due to the requirement that a compact set contain all of its limit points, global hyperbolicity can be stripped away from a spacetime through excising parts of the manifold, as Figure 6.4 illustrates.

Because of the excision of just a single point from the flat, two-dimensional spacetime pictured below, the set formed by  $J^+(p) \cap J^-(q)$  is no longer compact, and global hyperbolicity fails.

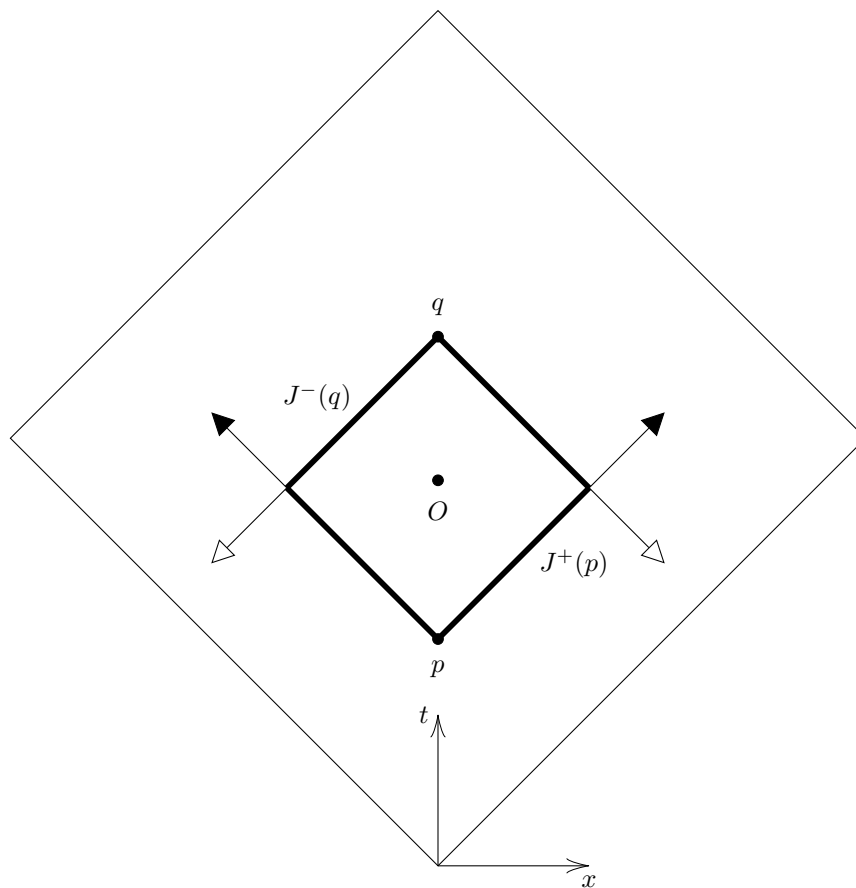


Figure 6.4: While a normal causal diamond would be globally hyperbolic, we have excised the origin in this diamond. With this limit point removed, the intersection of  $J^+(p)$  and  $J^-(q)$  is not compact and global hyperbolicity fails.

## Chapter 7

# Three Spacetimes and Two Causal Sets

In this section we undertake an analysis of three spacetimes, each with one time and one space dimension. We aim to use an analysis of these spacetimes to inform an answer to our question and frame an approach toward proving the *hauptvermutung* of Causal Set Theory.

In particular, we will identify how the three spacetimes are related, in terms of both their causal structure and their geometric structure. In this section we will focus on how a sprinkling with a fixed density produces causal sets faithfully embedded in the three spacetimes. A comparison of the causal structure of the three spacetimes will be conducted both according to the rungs of the causal ladder and a comparison of the causal sets which are faithfully embedded in each spacetime.

The three spacetimes are causal diamonds, which are, as in the previous section, flat and two-dimensional. The first,  $\mathcal{M}_1$  is a perfectly unaltered diamond. The second diamond,  $\mathcal{M}_2$  has a single point at its center excised. The third diamond,  $\mathcal{M}_3$  has a horizontal line of variable length  $l$  excised along the diagonal. We present these three spacetimes in Figure 7.1.

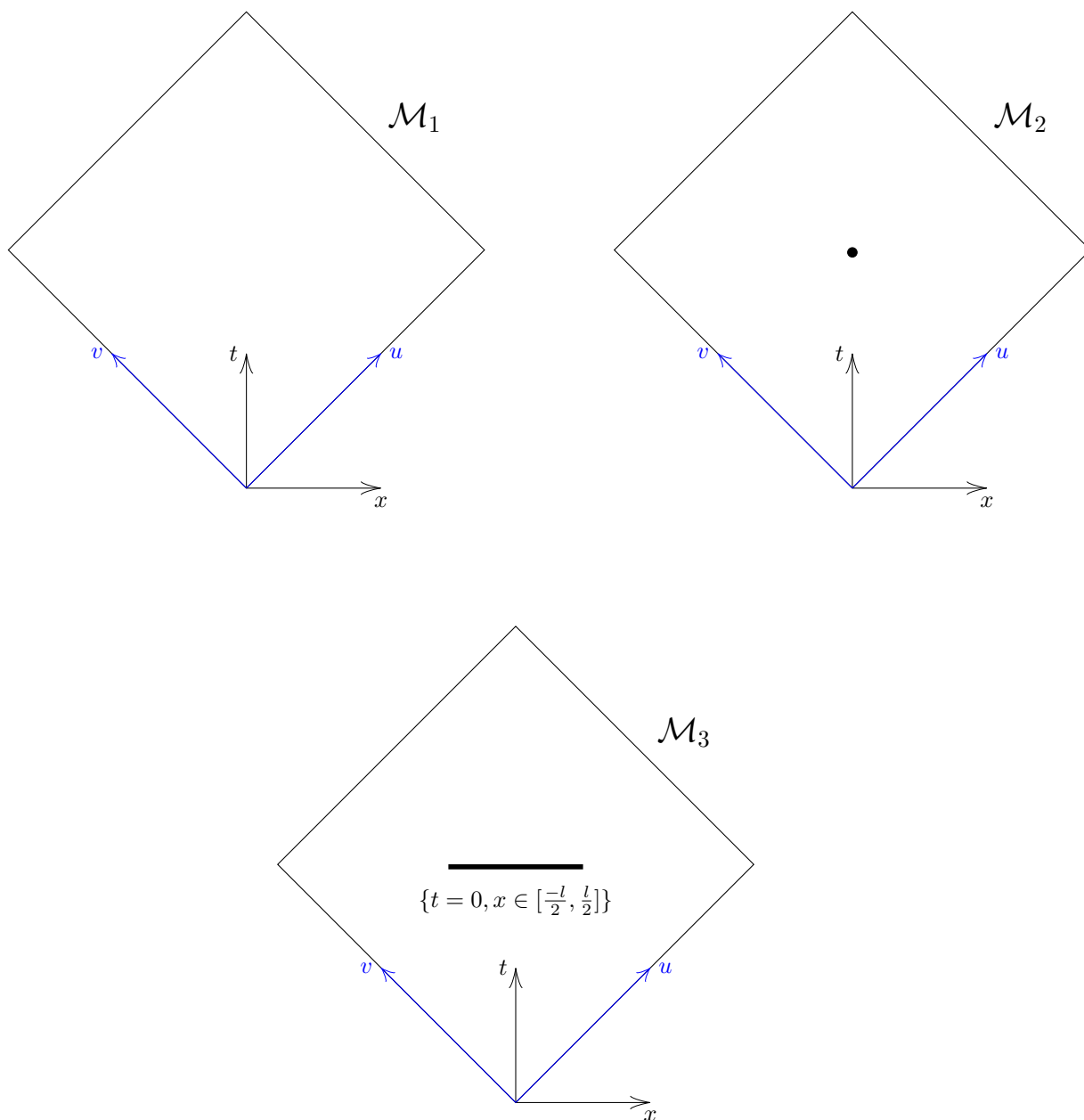


Figure 7.1: The three spacetimes in question. As stated,  $\mathcal{M}_1$  is an unaltered causal diamond.  $\mathcal{M}_2$  has its origin excised.  $\mathcal{M}_3$  has a strip excised.

The first task is to understand where the spacetimes  $\mathcal{M}_1$ ,  $\mathcal{M}_2$  and  $\mathcal{M}_3$  lie on the causal ladder.

## 7.1 Locating $\mathcal{M}_1$ , $\mathcal{M}_2$ , and $\mathcal{M}_3$ on the Causal Ladder

Recalling our discussion of Figure 6.4,  $\mathcal{M}_1$  is a diamond with no excisions, and so is globally hyperbolic.

As discussed, having even a single point in the interior missing precludes global hyperbolicity since causal intervals which enclose any part of the excision will not be compact. On the other hand, neither excision disallows the existence of arbitrarily small causally convex neighborhoods. So both  $\mathcal{M}_2$  and  $\mathcal{M}_3$  are strongly causal. Let us try and place the two spacetimes on one of the rungs between global hyperbolicity and strong causality.

We consider stable causality first. Recall that we can think of a spacetime as being stably causal if widening the lightcones in the spacetime would not allow for closed causal loops. While we do not go through finding an element of the class of conformal metrics which preserves the causality of  $\mathcal{M}_2$  and  $\mathcal{M}_3$  (in accordance with the formal definition of stable causality), we see that neither of these spacetimes is anywhere near allowing for closed causal loops. Widening the lightcones in either of these spacetimes will not alter the structure of the spacetimes in any appreciable way in regard to the admission of closed causal loops.

Next we consider causal continuity. Recall that a spacetime is causally continuous if the maps  $I^{+/-}$  are continuous and injective everywhere in the spacetime. Given that both of these spacetimes are strongly causal (and hence distinguishing), the maps  $I^{+/-}(p)$  are injective on both  $\mathcal{M}_2$  and  $\mathcal{M}_3$ . The excision of a single point in the spacetime  $\mathcal{M}_2$  does not affect the continuity of  $I^{+/-}(p)$ . However, the excision of a segment with non-zero length from  $\mathcal{M}_3$  does indeed make the maps  $I^{+/-}(p)$  discontinuous. Consider how the value of  $I^+(p)$  changes drastically as the point  $p$  is shifted infinitesimally in Figure 7.2.



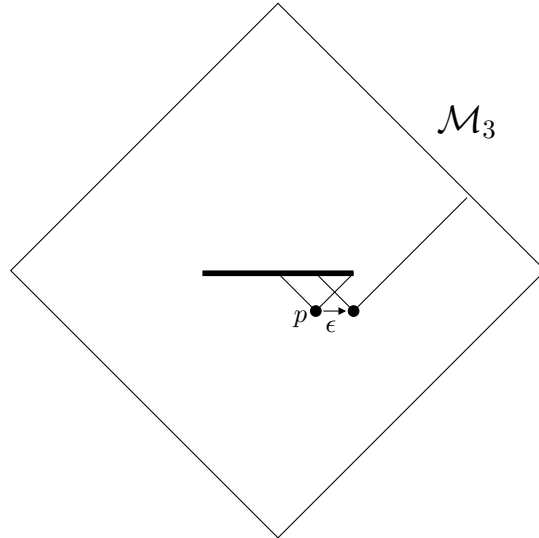


Figure 7.2: As we shift the point  $p$  by an arbitrarily small amount, the chronological future of  $p$  grows drastically, impeding the continuity of  $I^+(p)$ .

We see that as we approach the endpoints of the excision, the causal future of points below the excision grows to include an infinite number more points once one null line emanating from  $p$  is able to reach past the excision. This makes the map  $I^+(p)$  discontinuous. Hence  $\mathcal{M}_3$  is not causally continuous.

So  $\mathcal{M}_3$  is stably causal but not causally continuous. In fact, there are more rungs which lie between stable causality and causal continuity, but having separated  $\mathcal{M}_2$  and  $\mathcal{M}_3$  to this degree will suffice for our discussion.

$\mathcal{M}_1$  is globally hyperbolic,  $\mathcal{M}_2$  is causally continuous, and  $\mathcal{M}_3$  is stably causal. There may be a rung above stable causality and below causal continuity which  $\mathcal{M}_3$  occupies.

## 7.2 Poisson Sprinklings in the Three Diamonds

The causal diamonds are squares which can be described by  $(t, x)$  coordinates. Given that the edges are rotated from the  $(t, x)$  axes, we are motivated to introduce lightcone coordinates,  $(u, v)$ . Both sets of axes are labeled in Figure 7.3 below.

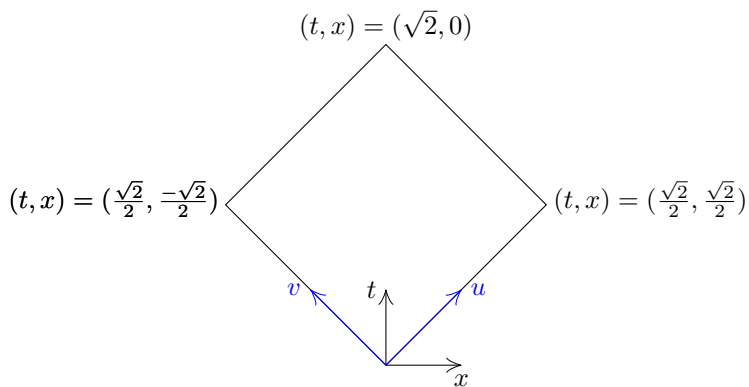


Figure 7.3: A diamond with  $(u, v)$  and  $(t, x)$  axes labeled, and the vertices of the diamond given in  $(t, x)$  coordinates.

The lightcone coordinates are given by

$$u = \frac{t+x}{\sqrt{2}}$$

$$v = \frac{t-x}{\sqrt{2}}.$$

This makes the diamond much easier to describe, as the ranges are simply  $u \in [0, 1]$  and  $v \in [0, 1]$ . We note that these coordinate ranges easily tell us that the maximum possible length of the excised segment is  $\sqrt{2}$ .

We will run a Poisson sprinkling in  $\mathcal{M}_1, \mathcal{M}_2$ , and  $\mathcal{M}_3$ . When the Poisson process is run on one of the spacetimes, it will return a random finite subset of that spacetime. By then sprinkling these points, they are endowed with the causal relationship they inherit from their manifold existence, and then abstracted from the manifold to become elements of an abstract causal set.

For now we choose to fix the density of our Poisson process to be

$$\rho = 10.$$

The area of each of the three spacetimes are the same and each equal 1. Technically,

$$\int_{\mathcal{M}_{1,2,3}} \sqrt{-g} \, dudv = 1.$$

Thus the Poisson distribution of interest is

$$\mathbb{P}(|X| = k) = \frac{(10)^k e^{-10}}{k!}.$$

This distribution produces an integer distributed according to the Poisson distribution with average value 10. Once this integer is produced, a corresponding

number of points are selected from the spacetime, uniformly at random, with the selection of one point independent from all the others.

By using the same points (elements of the manifold) to construct a causal set in each of the three spacetimes, we will be able to compare the causal structures of the three spacetimes, by assessing whether the same causal relations exist between points in  $\mathcal{M}_1$ ,  $\mathcal{M}_2$ , and  $\mathcal{M}_3$ .

Before turning to this comparison, let us see build some intuition for what a Poisson processes run on  $\mathcal{M}_1$  looks like.

### 7.2.1 Sprinkling in $\mathcal{M}_1$

In Figure 7.4 below are pictured the random finite subsets obtained via two Poisson processes on  $\mathcal{M}_1$ . The first comprises 5 points, and the second has 14. They should appear to be roughly distributed over the whole of the spacetime.

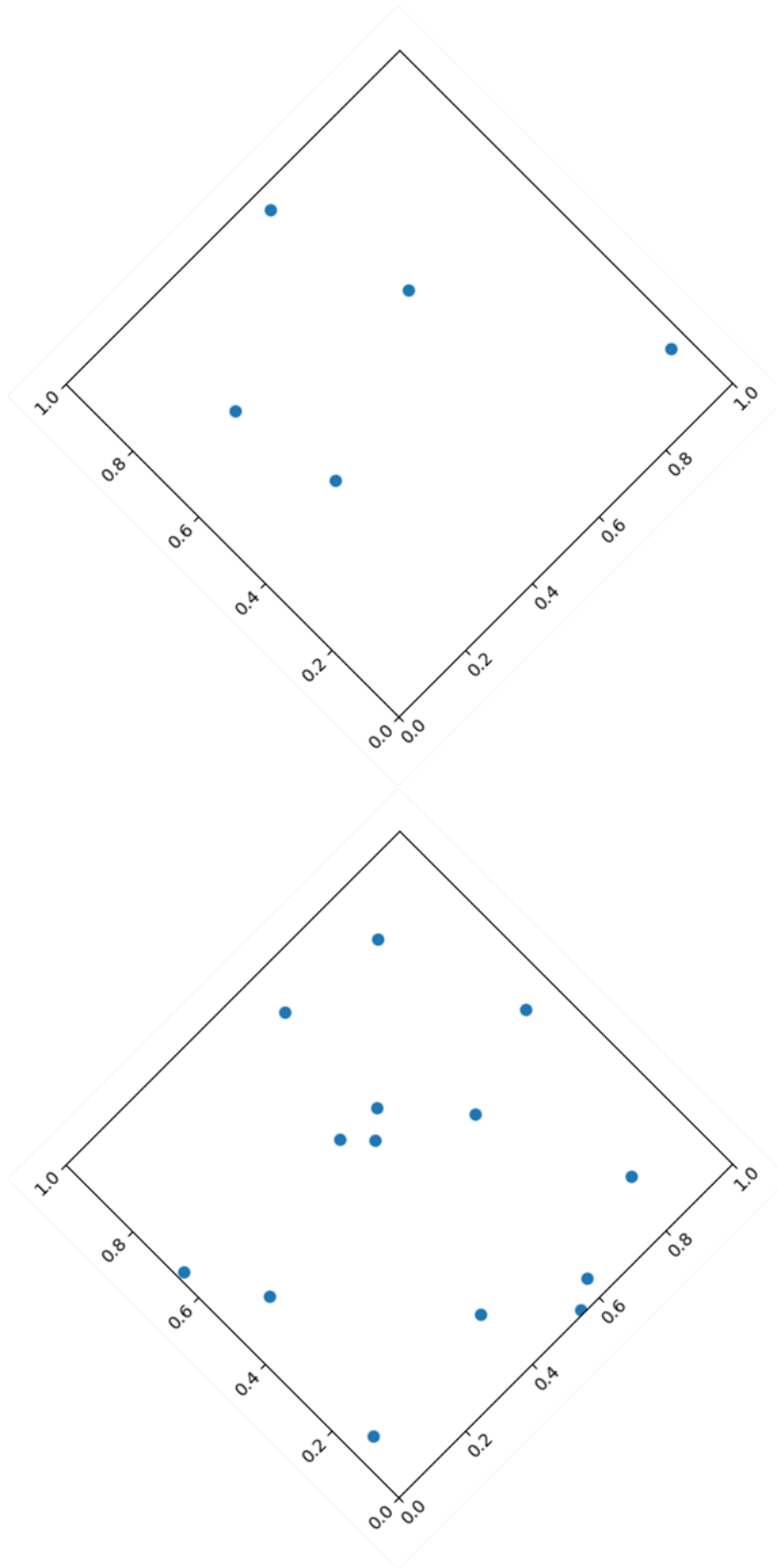


Figure 7.4: Two Poisson processes run on  $\mathcal{M}_1$ . The first process yielded 5 points, and the second contains 14. The points appear roughly uniformly distributed across the diamond.

With some intuition for what a Poisson process outputs when run on a manifold, let us visualize a sprinkling next. A sprinkling not only entails running the Poisson process, but also endows the points which it picks out with the causal relationship they inherit from their spacetime.

The causal relationships will be illustrated with a Hasse diagram. A Hasse diagram places a line (an edge in a transitive acyclic graph) between two points if they are causally related, but neglects to place a line if the causal relationship between two points is inferred by the transitivity of the partial order, as in Definition 25.

All causal relationships are depicted with a green edge. The first of the plots in Figure 7.5 is not a Hasse diagram. It shows every causal relationship between points, with redundancies included. The second plot is a Hasse diagram, the transitive reduction of the first. Causal relationships not explicitly plotted are inferred by transitivity.

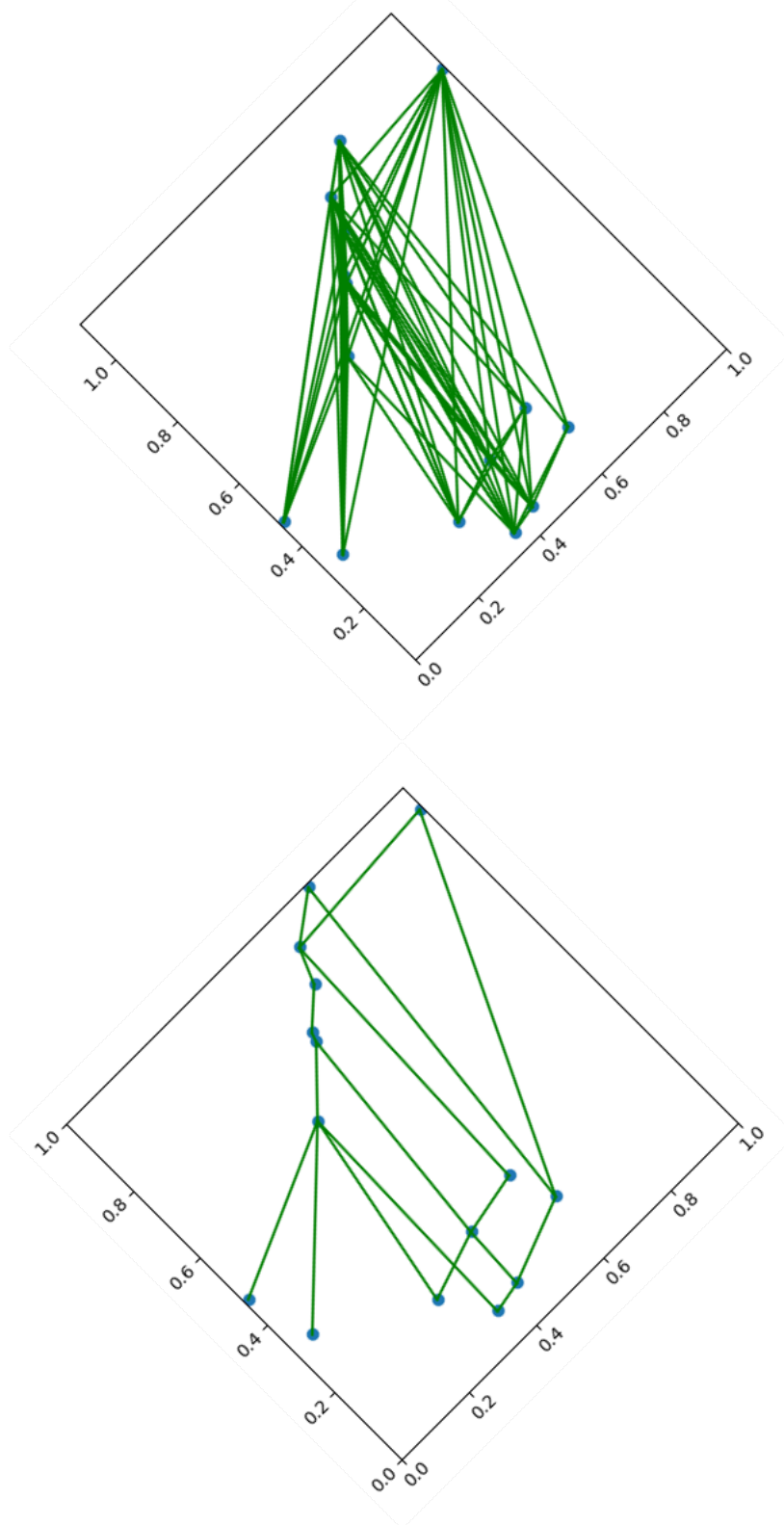


Figure 7.5: The first diagram pictured is a sprinkling of 15 points with each and every causal relationship marked by a green line joining causally related points. The second diagram is the transitive reduction of the one above it. Lines not pictured are inferred by the transitive property of the partial order.

### 7.2.2 Sprinkling in $\mathcal{M}_2$

Now let us examine the possible causal relationships for points sprinkled in  $\mathcal{M}_2$ . Recall that  $\mathcal{M}_2$  differs from  $\mathcal{M}_1$  by the excision of a single point.

We wish to compare the causal sets which are faithfully embedded in  $\mathcal{M}_2$  with those faithfully embedded in  $\mathcal{M}_1$ . We are prompted to ask whether this missing point in  $\mathcal{M}_2$  will impact the causal set which is sprinkled into this spacetime and cause it to differ from the causal set obtained by selecting the same finite subset of points from  $\mathcal{M}_1$ . We will conduct such a comparison by running a Poisson process on  $\mathcal{M}_1$ , and then sprinkling the points of  $\mathcal{M}_1$  which were selected by this process into  $\mathcal{M}_2$ . The causal relationships between these points, when they lie in  $\mathcal{M}_1$  and then in  $\mathcal{M}_2$  can then be compared.

An alteration to the causal set could occur in two places. Firstly, if the excised point were part of the finite subset selected by the Poisson process run on  $\mathcal{M}_1$ , then this point would have to be rejected in the causal set obtained on  $\mathcal{M}_2$ . Secondly, if the excised point prevented one point in the causal set on  $\mathcal{M}_2$  from communicating with another point in the causal set by blocking a causal curve joining the two points, then this causal relationship which existed in  $\mathcal{M}_1$  would be absent in  $\mathcal{M}_2$ . We address these two points as follows.

First, we can say with probability equal to 1 that the point taken away from  $\mathcal{M}_1$  will not be chosen as a point in the causal set because it has 0 area. That is,

$$\int_{origin} \sqrt{-g} \, dudv = 0.$$

and

$$\mathbb{P}(\text{any single point is selected}) = \frac{(0)^1 e^0}{1} = 0.$$

Second, because the excision is only a single point, with zero length (much less an area), any "line" which may have joined two causally related point can easily dodge the excision by making an indentation of arbitrarily small radius around the excised point, and still reach its desired destination. Importantly, the curve remains causal, so as to preserve the causal relationship that existed in  $\mathcal{M}_1$ .

We can see such an indentation in Figure 7.6 below.

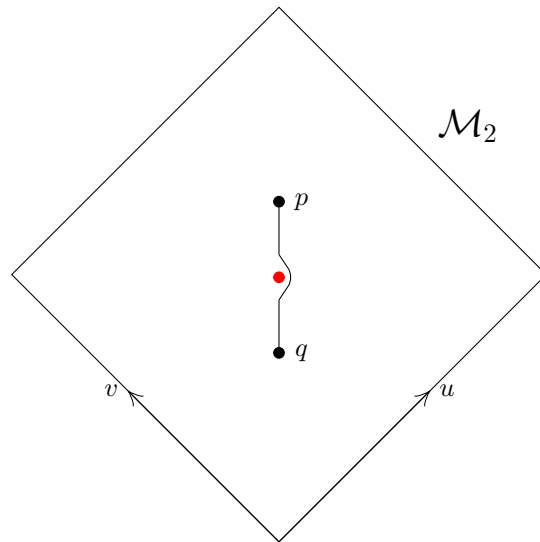


Figure 7.6: We can deform a line joining  $p$  to  $q$  by an arbitrarily small amount so as to preserve the causal relationship between the two points.

For these two reasons, the causal sets which can be faithfully embedded in  $\mathcal{M}_1$  and  $\mathcal{M}_2$  via a Poisson sprinkling are the same. Let us visualize this with Figure 7.7. It includes the Hasse diagrams on  $\mathcal{M}_1$  and  $\mathcal{M}_2$ . The causal sets are comprised of the same points selected from the two manifolds, and their causal relationships in each are depicted. For these two spacetimes, the causal relations are identical.



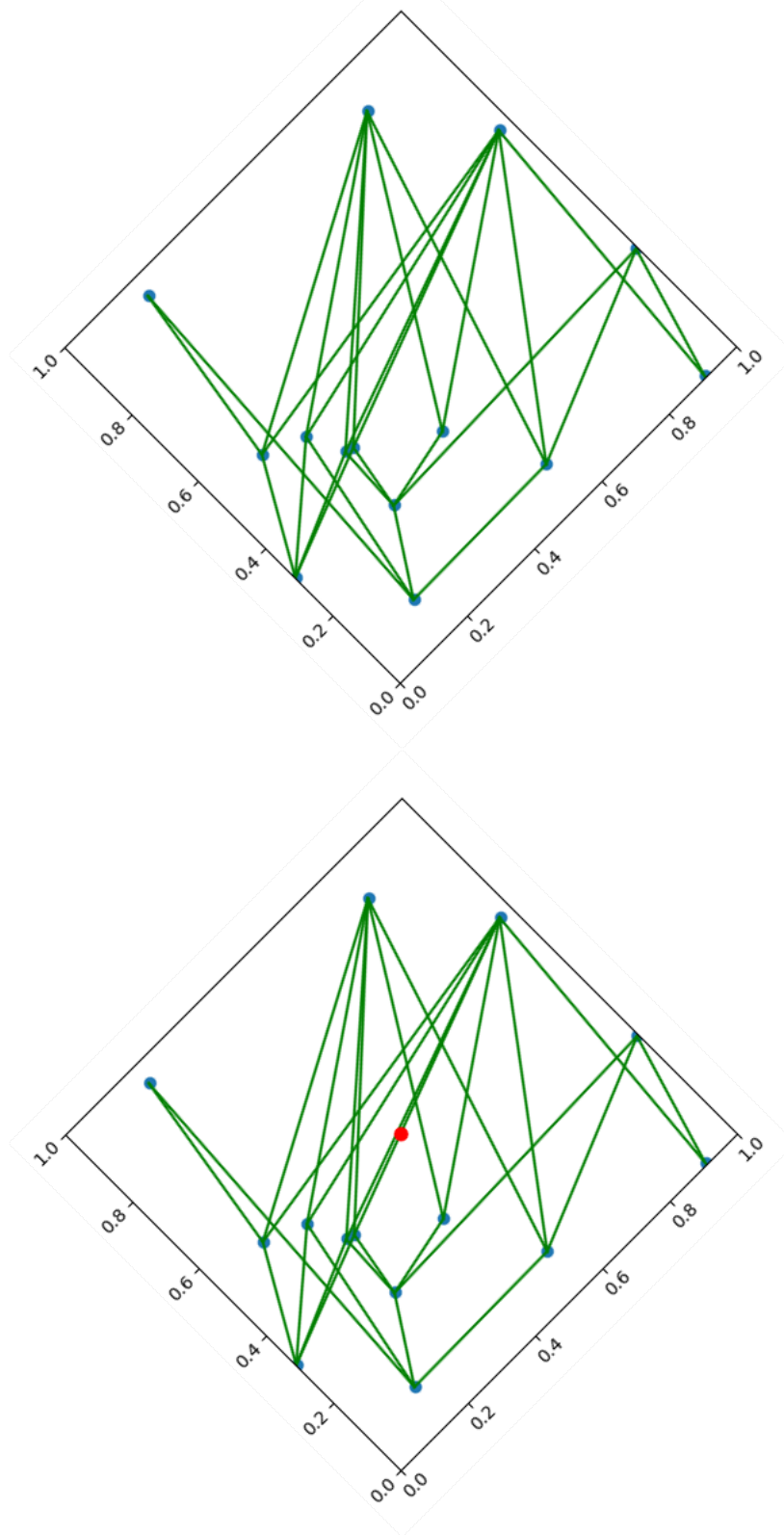


Figure 7.7: Pictured here are the Hasse diagrams for the same causal set faithfully embedded in  $\mathcal{M}_1$  and  $\mathcal{M}_2$ . The points selected as well as the causal relations between them are identical. Thus the two causal sets are indeed the same set.

By the reasoning and diagrams above, the spacetimes  $\mathcal{M}_1$  and  $\mathcal{M}_2$  allow for the same causal sets to be embedded in them. The *haupvermutung* of Causal Set Theory would now tell us that  $\mathcal{M}_1$  and  $\mathcal{M}_2$  are approximately isometric, and constitute the same “essentially unique” manifold. While the definition of an approximate isometry is deferred to the next chapter, we can make some comments here and see that the *haupvermutung* leads to a reasonable conclusion.

The excision in  $\mathcal{M}_2$  would preclude a global isometry from existing between  $\mathcal{M}_1$  and  $\mathcal{M}_2$ . One would not even be able to smoothly map one of these spacetimes into the other via a diffeomorphism due to this missing point. So, the notion of approximate isometry would need to allow for a loosening of the condition of smoothness in order to take into account this excision.

Additionally, paths in  $\mathcal{M}_2$  are not allowed to cross the excision. So the image of paths in  $\mathcal{M}_1$  which do cross it would need to be indented in  $\mathcal{M}_2$ . As we alluded to in our discussion of the causal relations in  $\mathcal{M}_2$ , however, the excision of only single point does allow paths to dodge this missing point with arbitrarily small indentations. So these indentations of paths which would otherwise cross the excision could be made arbitrarily small. Thus while their lengths may be more than their counterparts in  $\mathcal{M}_1$ , the difference in length could be made arbitrarily small.

If we can loosen the conditions of smoothness and absolute length-preservation in the ways discussed above, then it is reasonable to say that  $\mathcal{M}_1$  and  $\mathcal{M}_2$  are approximately isometric. We will discuss this with specific definitions in the next chapter.

Let us turn to  $\mathcal{M}_3$ , and compare the causal sets which can be faithfully embedded there, with those faithfully embedded in  $\mathcal{M}_1$ .

### 7.2.3 Sprinkling in $\mathcal{M}_3$

We recall that  $\mathcal{M}_3$  contains an excised line segment. We can observe fairly immediately that certain causal restrictions will be blocked. Figure 7.8 below gives a preliminary idea of one relation which would be allowed in  $\mathcal{M}_1$  but is blocked in  $\mathcal{M}_3$ .

From point  $p$ , one can travel on a causal curve to the point  $r$ , however the excision blocks a causal curve from ever joining  $p$  to  $q$ . So any causal set sprinkled in  $\mathcal{M}_1$  containing the points  $p, q$  and  $r$  would not be the same as the causal set obtained from  $\mathcal{M}_3$  which contains  $p, q$  and  $r$  as elements.

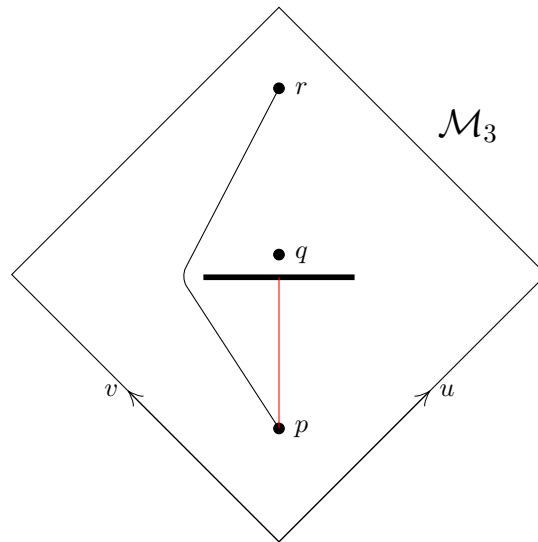


Figure 7.8: In  $\mathcal{M}_3$ , the point  $q$  is too close to the excision to be reached by point  $p$  via a causal curve. The point  $r$ , however, is a suitable distance above the excision, and so is causally related to  $p$ .

In fact, there are four disjoint regions of  $\mathcal{M}_3$  which are restricted in regard to other points of the spacetime which they can be causally related to as a result of the excision.

We can visualize the restricted regions, and which points can access them in Figure 7.9 below. In each of the four regions below the excision is plotted a sample point. From each of these same points emanate two null lines. Some null lines run into the excision, in which case they terminate. If a null line reaches above the excision, then it is taken null along the alternate axis until it reached the boundary of the spacetime. In some cases a path perpendicular to the excision is also plotted to help give a feeling for where on the spacetime these points lie.

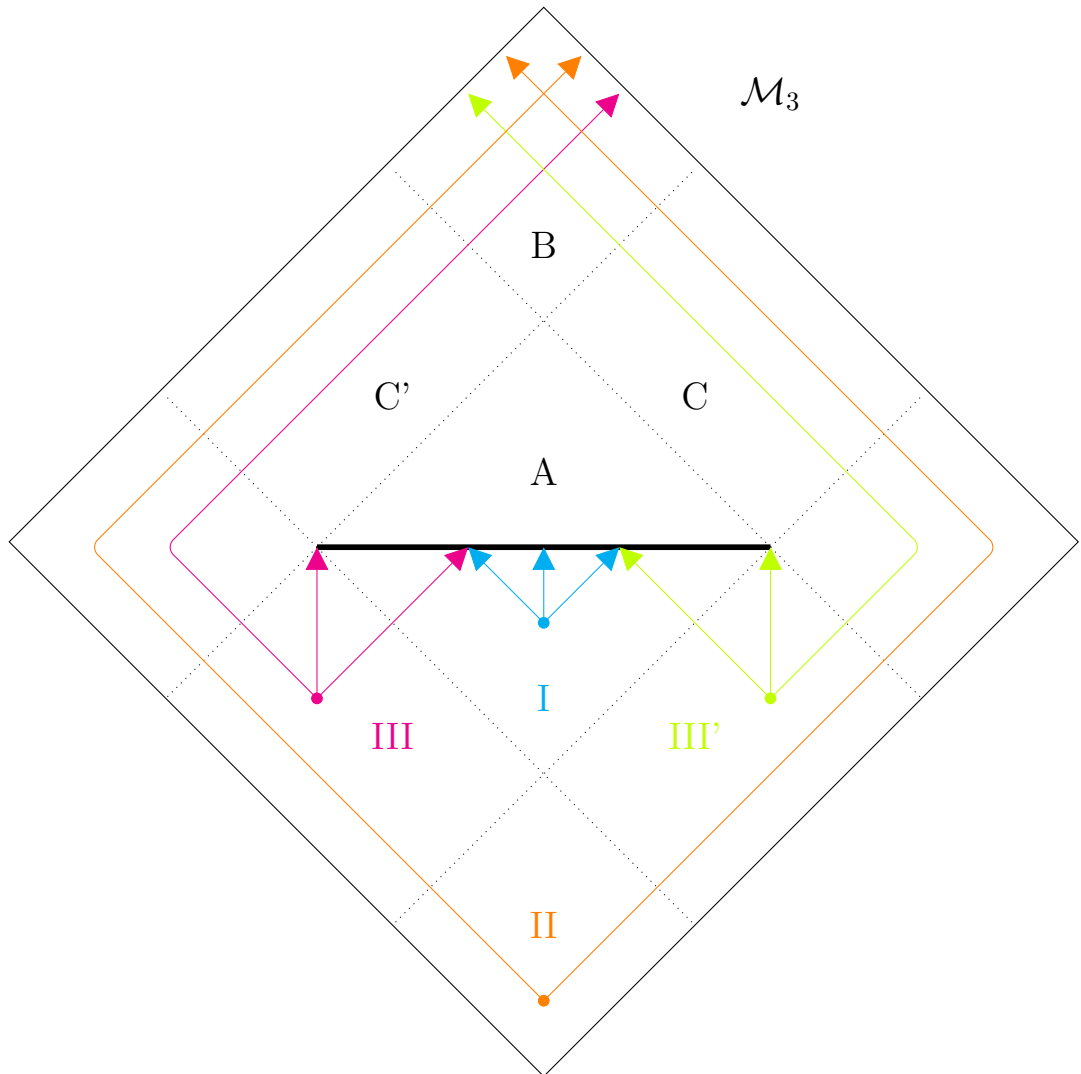


Figure 7.9: A schematic of spacetime  $\mathcal{M}_3$  depicting sample points in each restricted region and curves which reflect the points which are causally reachable from within each region.

Let us formalize this. In the following, we will use the notation  $p_I$ ,  $p_{II}$ , etc. to denote a point in region I, II, respectively. Additionally,  $J_{\mathcal{M}_i}^{+/-}(q)$  will be taken as the future or past of  $q$  as it would be in  $\mathcal{M}_i$ , for  $i = 1, 2, 3$ .

Then we have the following potential relations.

$$\begin{aligned} J_{\mathcal{M}_3}^+(p_I) &= J_{\mathcal{M}_1}^+(p_I) \cap I \\ J_{\mathcal{M}_3}^+(p_{II}) &= J_{\mathcal{M}_1}^+(p_{II}) \cap (C \cup C' \cup B) \\ J_{\mathcal{M}_3}^+(p_{III}) &= J_{\mathcal{M}_1}^+(p_{III}) \cap (C' \cup B) \\ J_{\mathcal{M}_3}^+(p_{III'}) &= J_{\mathcal{M}_1}^+(p_{III'}) \cap (C \cup B) \end{aligned}$$

A point in  $\mathcal{M}_3$  which is not an element of any of regions I, II, III, or III', has as its causal future the same set of points as it would in  $\mathcal{M}_1$ . That is,

$$J_{\mathcal{M}_3}^+(q) = J_{\mathcal{M}_1}^+(q) \quad \forall q \notin (I \cup II \cup III \cup III')$$

We also note that no point outside of region A can reach any point in region A via a future directed causal curve. That is,

$$J_{\mathcal{M}_3}^-(r) = J_{\mathcal{M}_1}^-(r) \cap A \quad \forall r \in A$$

Given this analysis, let us consider the Hasse diagram on  $\mathcal{M}_3$  for the same set of points selected in  $\mathcal{M}_1$  and  $\mathcal{M}_2$ , and see how the causal relationship (and the resulting causal set) changes.

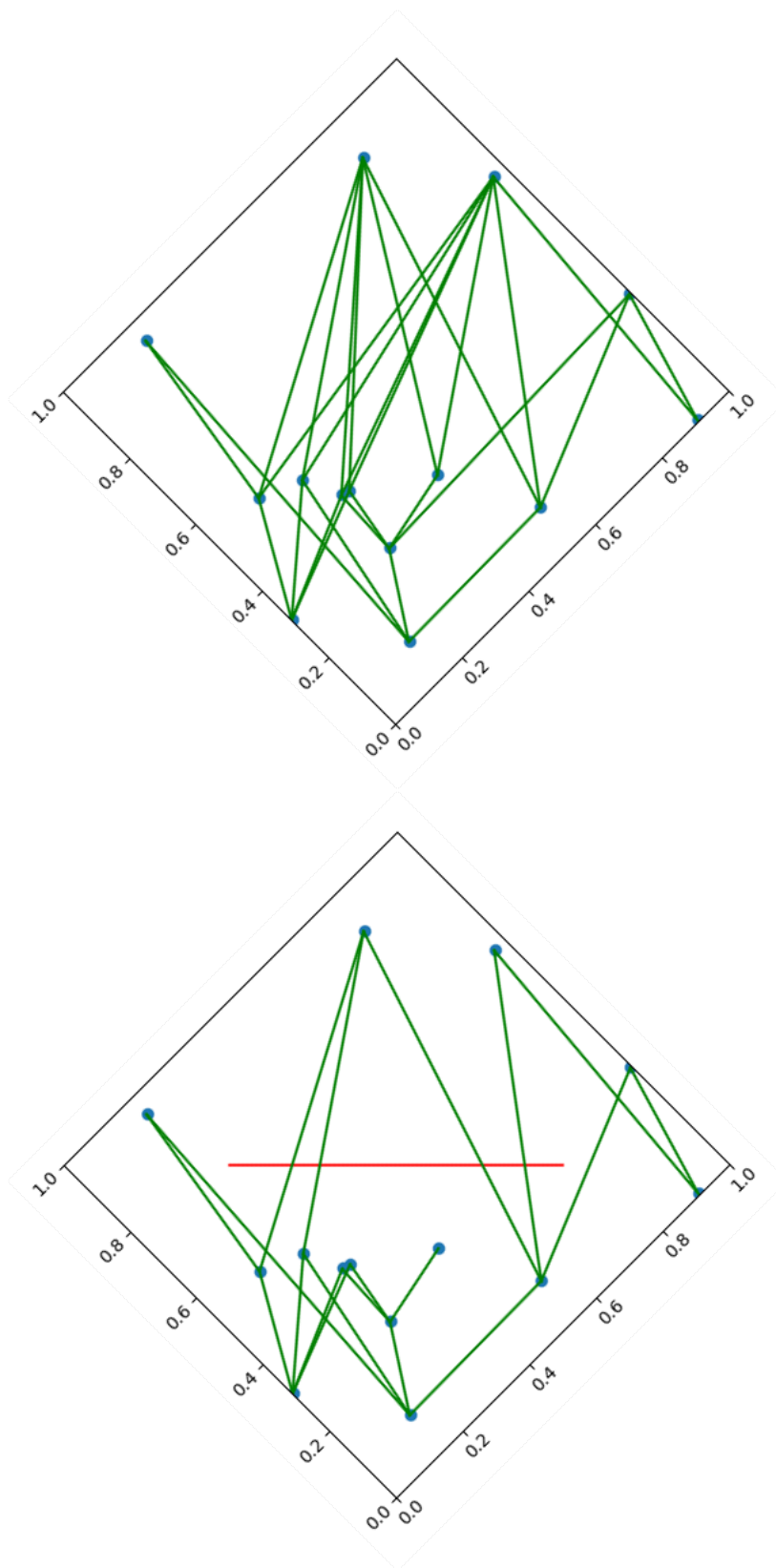


Figure 7.10: A Hasse diagram illustrating causal connections for a causal set obtained from  $\mathcal{M}_3$ . at the bottom. At top is pictured for reference the causal set using the same elements sprinkled in  $\mathcal{M}_1$ .

And so at a density of 10 and length of the excision of  $l = \frac{\sqrt{2}}{2}$ , this is the causal set faithfully embedded in  $\mathcal{M}_3$  obtained by using the same points we used in  $\mathcal{M}_1$  and  $\mathcal{M}_2$ . The number of edges in the Hasse diagram for  $\mathcal{M}_3$  is less than the number for the corresponding diagram on  $\mathcal{M}_1$ . In particular, our image allows us to see that points in region I are no longer related to points above the excision, while these relations did exist in  $\mathcal{M}_1$ . We also see that in  $\mathcal{M}_3$ , the points above the excision have fewer edges connecting them to other points in the causal set

We will attempt to describe the number of relations which exist in  $\mathcal{M}_1$  will be blocked in  $\mathcal{M}_3$  due to the excision in the next subsection.

### 7.2.4 The Probability of a Blocked Relation

We wish to compare the causal sets obtained on  $\mathcal{M}_3$  with those obtained in  $\mathcal{M}_1$ . As we have seen, the potential differences are dependent on selected points falling within the restricted regions, and furthermore are dependent on other points being selected in regions which are inaccessible to those regions, but which would have comprised part of the causal future of the original point had they been in  $\mathcal{M}_1$ .

The probability that we select points in restricted regions and also select other inaccessible points is a function of (1) the areas of the restricted regions and (2) the density at which we sprinkle.

The areas of the restricted regions, I, II, III and III' all depend on the length of the excision, as we can observe with a simple image. The null lines which form the dividing markers of the regions have their starting and ending points altered so as to change the areas of the four restricted regions.

As a function of the length,  $l$  of the excision, the areas of the regions are calculated to be the following.

$$\begin{aligned} Area(\text{I}) &= \frac{l^2}{4} = Area(A) \\ Area(\text{II}) &= \frac{l^2 - 2\sqrt{2}l + 2}{8} = Area(B) \\ Area(\text{III}) = Area(\text{III}') &= \frac{l(\sqrt{2} - l)}{4} = Area(C) = Area(C') \end{aligned}$$

We can visualize the areas of these regions with Figure 7.11 below.

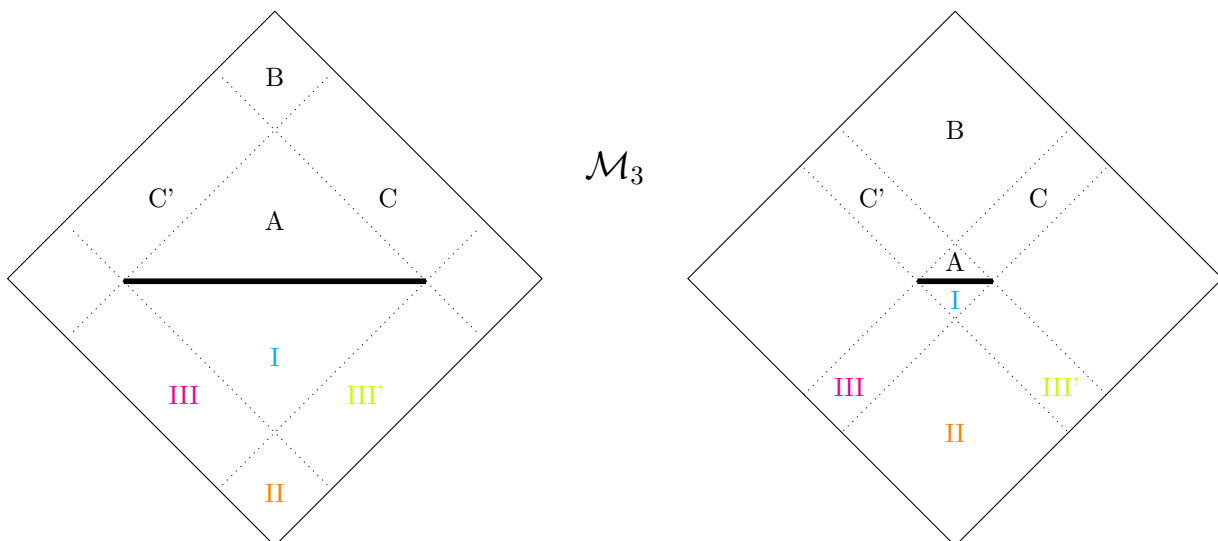


Figure 7.11: Two illustrations of the spacetime  $\mathcal{M}_3$  with varying lengths of the excision, and the corresponding restricted regions drawn in each case.

Let us also label the excision and endpoints in  $(u, v)$ -coordinates in Figure 7.12.

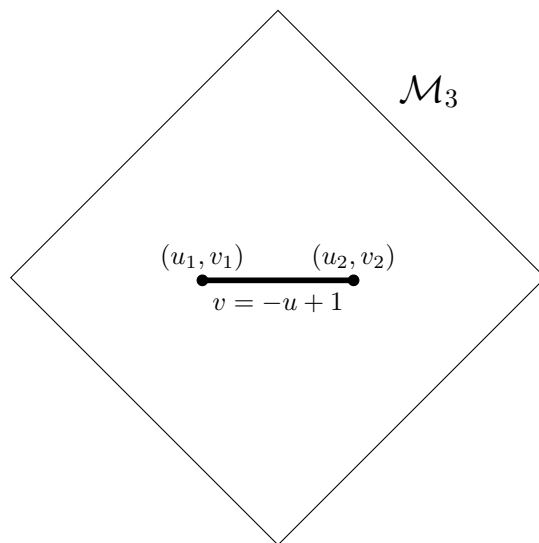


Figure 7.12: A labeling of the parts of the excision in  $\mathcal{M}_3$ . The left endpoint of the excision is  $(u_1, v_1)$ , its right endpoint is  $(u_2, v_2)$ . The excision is a segment coming from the line  $v = -u + 1$ .



We are interested in understanding how many blocked relations  $\mathcal{M}_3$  will have. By a blocked relation, we mean a relation between two points which would exist in  $\mathcal{M}_1$  but which does not exist between the same points in  $\mathcal{M}_3$  due to the excision.

To do this, we will treat the number of relations as a random variable. Recalling that the Poisson distribution is the limit of the binomial distribution, we imagine discretizing a spacetime into cells, and assigning the probability of placing a point in each cell via a Poisson distribution as follows.

$$\mathbb{P}(\text{point in cell } i) = \rho dV_i,$$

where  $dV_i$  is the volume element corresponding to cell  $i$ .

The number of relations in  $\mathcal{M}_1$  is given by

$$N(R) = \sum_{i \in \mathcal{M}_1} \chi_i \sum_{j \in (J^+(i) \cap \mathcal{M}_1)} \chi_j,$$

where  $\chi_i$  is the characteristic function, taking the value 1 if cell  $i$  is populated and 0 otherwise.

In this way, we can calculate the number of blocked relations by, starting with region I for example,

$$N(BR) = \sum_{i \in I} \chi_i \sum_{j \in (J^+(i) \cap \text{blocked regions})} \chi_j.$$

We can then compute the expected value of the number of relations or blocked relations as an integral. We give a calculation of the expected value of the number of relations in  $\mathcal{M}_1$  to give a sense for the calculation.

$$\begin{aligned} \langle N(R) \rangle &= \rho^2 \int_{\mathcal{M}_1} d^2p \int_{J^+(p \cap \mathcal{M}_1)} d^2q \\ &= \rho^2 \int_0^1 du_p \int_0^1 dv_p (1 - u_p)(1 - v_p) \\ &= \rho^2 \left(1 - 1 + \frac{1}{4}\right) \\ &= \frac{\rho^2}{4}. \end{aligned}$$

As we move to compute the expected values of the number of blocked relations, we use the notation  $N(BR)_{I, A \cup C \cup C' \cup B}$  to denote the number of relations resulting from picking a point  $p$  in region I and a point  $q$  in  $A \cup C \cup C' \cup B$  which would be related if not for the excision.

There are four contributions to  $N(BR)$ , coming from  $N(BR)_{I, A \cup C \cup C' \cup B}$ ,  $N(BR)_{II, A}$ ,  $N(BR)_{III, A \cup C}$ , and  $N(BR)_{III', A \cup C'}$ . We will compute each of these four expectation values and then add them to obtain  $\langle N(BR) \rangle$ .

$$\begin{aligned}
\langle N(BR)_{\text{I}, A \cup C \cup C' \cup B} \rangle &= \rho^2 \int_{\text{I}} d^2 p \int_{J^+(p) \cap (A \cup C \cup C' \cup B)} d^2 q \\
&= \rho^2 \int_{\text{I}} du_p dv_p [J^+(p) \cap (\text{Area}(A) \cup \text{Area}(C) \cup \text{Area}(C') \cup \text{Area}(B))] \\
&= \rho^2 \int_{u_1}^{u_2} du_p \int_{v_2}^{-u_p+1} dv_p [(1-u_p)(1-v_p) - \frac{1}{2}(1-u_p-v_p)^2] \\
&= \rho^2 \int_{u_1}^{u_2} du_p [\frac{2}{3}u_p^3 + \frac{1}{6}v_2^3 - u_p^2 + \frac{1}{2}(u_p^2-1)v_2 + \frac{1}{3}] \\
&= -\frac{\rho^2}{6} [u_1^4 - u_2^4 + u_1 v_2^3 - u_2 v_2^3 - 2u_1^3 + 2u_2^3 + (u_1^3 - 3u_1)v_2 \\
&\quad - (u_2^3 - 3u_2)v_2 + 2u_1 - 2u_2]
\end{aligned}$$

$$\begin{aligned}
\langle N(BR)_{\text{II}, A} \rangle &= \rho^2 \int_{\text{II}} d^2 p \int_{J^+(p) \cap A} d^2 q \\
&= \rho^2 \int_{\text{II}} du_p dv_p \text{Area}(A) \\
&= \rho^2 \int_0^{u_1} du_p \int_0^{v_1} dv_p \frac{(\sqrt{2}(v_1-v_2))^2}{4} \\
&= \rho^2 u_1 v_1 \frac{(v_1-v_2)^2}{2}
\end{aligned}$$

$$\begin{aligned}
\langle N(BR)_{\text{III}, A \cup C} \rangle &= \int_{\text{III}} d^2 p \int_{J^+(p) \cap (A \cup C)} d^2 q \\
&= \rho^2 \int_{\text{III}} du_p dv_p [J^+(p) \cap (\text{Area}(A) \cup \text{Area}(C))] \\
&= \rho^2 \int_0^{u_1} du_p \int_{v_2}^{v_1} dv_p [(v_1-v_p)(1-u_1-v_1+v_p) + \frac{1}{2}(v_1-v_p)^2] \\
&= \rho^2 \int_0^{u_1} du_p [-\frac{1}{2}(u_1-1)v_1^2 - \frac{1}{6}v_1^3 - \frac{1}{2}(u_1+v_1-1)v_2^2 + \frac{1}{6}v_2^3 \\
&\quad + \frac{1}{2}(2(u_1-1)v_1 + v_1^2)v_2] \\
&= -\frac{\rho^2 u_1}{6} [3(u_1-1)v_1^2 + v_1^3 + 3(u_1+v_1-1)v_2^2 - v_2^3 \\
&\quad - 3(2(u_1-1)v_1 + v_1^2)v_2]
\end{aligned}$$

$$\langle N(BR)_{\text{III}, A \cup C'} \rangle = \langle N(BR)_{\text{III}, A \cup C} \rangle$$

So we arrive at the result that

$$\begin{aligned}
\langle N(BR) \rangle &= \langle N(BR)_{I,AUCUC'UB} \rangle + \langle N(BR)_{II,A} \rangle + \langle N(BR)_{III,AUC} \rangle + \langle N(BR)_{III',AUC'} \rangle \\
&= -\frac{\rho^2}{6} [u_1^4 - u_2^4 + u_1 v_2^3 - u_2 v_2^3 - 2u_1^3 + 2u_2^3 + (u_1^3 - 3u_1)v_2 \\
&\quad - (u_2^3 - 3u_2)v_2 + 2u_1 - 2u_2] + \rho^2 u_1 v_1 \frac{(v_1 - v_2)^2}{2} - \frac{\rho^2 u_1}{3} [3(u_1 - 1)v_1^2 \\
&\quad + v_1^3 + 3(u_1 + v_1 - 1)v_2^2 - v_2^3 - 3(2(u_1 - 1)v_1 + v_1^2)v_2].
\end{aligned}$$

Now substituting

$$\begin{aligned}
u_1 &= \frac{\sqrt{2} - l}{2\sqrt{2}} \\
u_2 &= \frac{\sqrt{2} + l}{2\sqrt{2}} \\
v_1 &= \frac{\sqrt{2} + l}{2\sqrt{2}} \\
v_2 &= \frac{\sqrt{2} - l}{2\sqrt{2}}
\end{aligned}$$

gives  $\langle N(BR) \rangle$

$$\begin{aligned}
&= -\frac{1}{32} (l + \sqrt{2})(l - \sqrt{2})l^2 \rho^2 + \frac{1}{768} [2(l + \sqrt{2})^4 - 2(l + \sqrt{2})(l - \sqrt{2})^3 - 4(l - \sqrt{2})^4 \\
&\quad - 8\sqrt{2}(l + \sqrt{2})^3 - 8\sqrt{2}(l - \sqrt{2})^3 - \sqrt{2}(\sqrt{2}(l + \sqrt{2})^3 - 24\sqrt{2}(l + \sqrt{2}))(l - \sqrt{2}) \\
&\quad - \sqrt{2}(\sqrt{2}(l - \sqrt{2})^3 - 24\sqrt{2}(l - \sqrt{2}))(l - \sqrt{2}) + 64\sqrt{2}(l + \sqrt{2}) + 64\sqrt{2}(l - \sqrt{2}) \\
&\quad + \frac{1}{384} (4(l - \sqrt{2})^4 + 8\sqrt{2}(l - \sqrt{2})^3 + \sqrt{2}(\sqrt{2}(l - \sqrt{2})^3 - 24\sqrt{2}(l - \sqrt{2}))(l - \sqrt{2}) \\
&\quad - 64\sqrt{2}(l - \sqrt{2}))] \rho^2.
\end{aligned}$$

This simplifies to give

$$\langle N(BR) \rangle = -\frac{\rho^2}{192} [5l^4 + 4\sqrt{2}l^3 - 12l^2 - 16\sqrt{2}l - 12].$$

The expected number of blocked relations as a function of the density,  $\rho$  and the length of the excision  $l$  simplified nicely into an expression quartic in  $l$  and quadratic  $\rho$ . The function is positive for small values of  $l$ , and importantly is positive for  $l \in [0, \sqrt{2}]$ , since  $\sqrt{2}$  is the maximum possible length of the excision.

We first note that keeping  $l$  constant and taking  $\rho \rightarrow \infty$  leads to a divergence. This is expected. If we sprinkle at an extremely high density, then we will obtain

more points in the restricted regions (and in all regions) and thus obtain more blocked relations.

We can consider taking the ratio  $\frac{\langle N(BR) \rangle}{\langle N(R) \rangle}$  where  $\langle N(R) \rangle$  is simply the number of relations expected in  $\mathcal{M}_1$ , calculated previously to be  $\frac{\rho^2}{4}$ . Then dependence on the density drops out, in exchange for a factor of 4, giving

$$\frac{\langle N(BR) \rangle}{\langle N(R) \rangle} = -\frac{1}{48}[5l^4 + 4\sqrt{2}l^3 - 12l^2 - 16\sqrt{2}l - 12].$$

It is helpful in addition to take the limit as the length of the excision takes the largest value it can (cutting across the entire diamond). We obtain

$$\lim_{l \rightarrow \sqrt{2}} \langle N(BR) \rangle = \frac{1}{6}\rho^2,$$

so that comparing with the number of relations expected in  $\mathcal{M}_1$  gives

$$\lim_{l \rightarrow \sqrt{2}} \frac{\langle N(BR) \rangle}{\langle N(R) \rangle} = \frac{2}{3}.$$

We give a brief illustration of what the diamond would look like with such an excision in Figure 7.13.

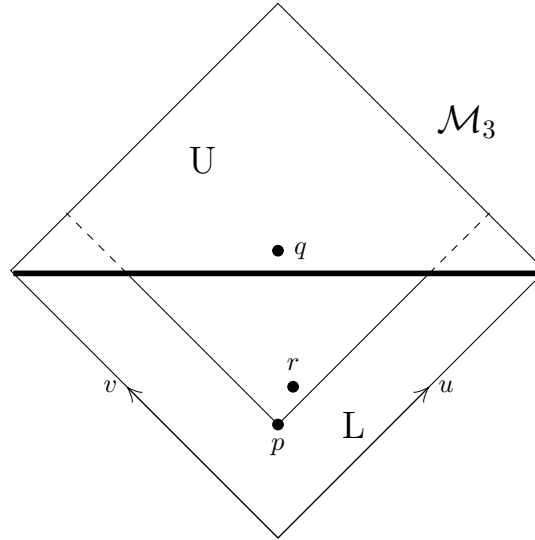


Figure 7.13: The excision here divides  $\mathcal{M}_3$  into two halves. The upper half is labeled  $U$ , the lower half,  $L$ . A point  $q$  has a blocked relation with  $p$ , while  $r$  is still causally related to  $p$  as it would have been in  $\mathcal{M}_1$ .

Of course the dropping out of the density accounts for the fact that density would be kept the same in the two scenarios in order to make a sensible comparison. This limit seems to tell us that the number of blocked relations in  $\mathcal{M}_2$  will be  $\frac{2}{3}$  the number of total relations on  $\mathcal{M}_1$ , when the length of the excision is  $\sqrt{2}$ , the length of the diagonal.

If the causal diamond of  $\mathcal{M}_3$  has an excision along its diagonal, it is essentially split into two disconnected parts. The probability that a point is sprinkled in either of the halves should be the same, about  $\frac{1}{2}$ . If this first point is sprinkled in the top half of the diamond, then it has no blocked relations in its causal future.

If this sprinkled point is in the bottom half of the diamond, a blocked relation only arises if the next sprinkled point is in the top half. Otherwise, the relation is still a valid one in  $\mathcal{M}_3$ . That is to say, since  $q \in J^+(p) \cap U$ , there is a blocked relation between  $q$  and  $p$ . By contrast, since  $r \in J^+(p) \cap L$ , there is no blocked relation here.

This brings to light the fact that blocked relations not only depend on a point being sprinkled in the lower region  $L$ , but they also depend on where in  $L$  the point is sprinkled. As we can see in Figure 7.13, the point  $p$  will have more blocked relations with points in the upper half than the point  $r$  does. This is because the causal future of  $p$  includes more points in the lower half than does the point  $r$ , because  $r$  is closer to the excision than  $p$ . That is to say,

$$(J^+(r) \cap L) \subset (J^+(p) \cap L).$$

Coming back to our limit and ratio, we are being told that, of the total relations which are in tact in  $\mathcal{M}_1$ ,  $\frac{2}{3}$  of them will become blocked in  $\mathcal{M}_3$ .

This is indeed the majority of relations, and is sufficient basis to say that the causal sets which can be faithfully embedded in  $\mathcal{M}_1$  and  $\mathcal{M}_3$  are not the same. The causal set embedded in  $\mathcal{M}_1$  will in general have many more causal relations between its elements than do the same elements of a causal set in  $\mathcal{M}_3$ .

The *hauovermutung* of Causal Set Theory would tell us that the spacetimes  $\mathcal{M}_1$  and  $\mathcal{M}_3$  are not approximately isometric, and do not constitute the same essentially unique manifold. This seems like a reasonable conclusion. In the case that  $l = \sqrt{2}$ , these spacetimes are drastically different, but even when  $l$  is less than the full length of the diagonal, there are curves which would need to be indented a non-trivial amount in order to avoid the excision. These indentations cannot be made arbitrarily small as with the indentations made to avoid  $\mathcal{M}_2$ 's single-point excision. There would be a minimum, non-zero length that would need to be added to a curve which would have passed through the excision, in order for the curve to go around it. So the *hauovermutung* seems to hold for  $\mathcal{M}_1$  and  $\mathcal{M}_3$ : they do not give rise to the same faithfully embedded causal set, and they do not appear approximately isometric.

More detailed discussion of approximate isometries will come in the next chapter, and connections will be made to  $\mathcal{M}_1$ ,  $\mathcal{M}_2$ , and  $\mathcal{M}_3$ .

## Chapter 8

# Toward Identifying Essential Uniqueness

In this chapter, we work toward finding a more precise formulation of the portion of the *hauptvermutung* involving essential uniqueness. Let us briefly recall that we gave three possible formulations of the *hauptvermutung*. They were the following (here we will use  $\mathcal{N}$  to denote generic spacetimes so as not to confuse with the specific sample spacetimes of the previous chapter).

1. The same causal set,  $C$  can be faithfully embedded in two manifolds,  $\mathcal{N}_1$  and  $\mathcal{N}_2$  if and only if  $\mathcal{N}_1$  and  $\mathcal{N}_2$  constitute the same essentially unique manifold [18].
2. The same causal set,  $C$  can be faithfully embedded in two manifolds,  $\mathcal{N}_1$  and  $\mathcal{N}_2$  if and only if  $\mathcal{N}_1$  and  $\mathcal{N}_2$  are approximately isometric [17].
3. Given the space of all Lorentzian geometries,  $\mathcal{L}$  and denoting approximate isometry by  $\sim$  there is a correspondence between the quotient space  $\mathcal{L}/\sim$  and  $\Omega_C$ , where  $\Omega_C$  is the space of all causal sets which have manifold approximations [17].

The notion of essential uniqueness in statement 1 is discussed slightly in [18], where the authors assert that two manifolds with the same faithfully embedded causal set should be related via a diffeomorphism which preserves the causal set and which is an approximate isometry. Following Surya’s phrasing in statement 2, the notion of an “approximate isometry” thus seems to be the central means of identifying essential uniqueness, and will be the subject of this chapter.

Statement 3, also due to Surya, hints at considering the moduli space of Lorentzian geometries. Definitions involving such a space will be made use of in the following two sections, and a method for determining isometries between elements of such a moduli space will be discussed in section 8.2.

Noldus and Bombelli have made some progress towards defining approximate isometries, as well as towards constructing conditions for the existence of

isometries between Lorentzian manifolds in such papers as [19] and [20]. We will outline their work. We begin by following Bombelli and Noldus' construction of an approximate, or rather, an  $\epsilon$ -isometry.

We will outline these two paths, as they both make use of certain causal restrictions which may shed light on our ultimate question, in addition to suggesting unique viable paths forward to proving the *hauptvermutung*.

## 8.1 $\epsilon$ -Isometries

We begin with a few definitions which give new tools to describe distance in spacetime.

**Definition 55.** [20] *Given a set  $X$ , a function  $d : X \times X \rightarrow \mathbb{R}^+ \cup \{\infty\}$  is a Lorentz distance if for any  $x, y, z \in X$ ,  $d$  satisfies*

1.  $d(x, x) = 0$
2.  $d(x, y) > 0 \Rightarrow d(y, x) = 0$
3. (reverse triangle inequality)  $d(x, z) \geq d(x, y) + d(y, z)$  if  $d(x, y)d(y, z) > 0$ .

Noldus states that the canonical Lorentz distance on a chronological spacetime  $(\mathcal{M}, g)$  is defined as

**Definition 56.** [20]  $d_g := \sup_{\gamma} \{|\gamma|\}$ .

Here  $\gamma$  is a timelike future oriented causal curve with endpoints  $x$  and  $y$ . Furthermore, Bombelli and Noldus state that  $d_g$  is continuous and finite if and only if  $(\mathcal{M}, g)$  is globally hyperbolic.

**Definition 57.** [20] *Given a Lorentz distance function  $d$  which is continuous in the Alexandrov topology, the strong metric  $D$  on a set  $\mathcal{M}$  is defined by*

$$D(p, q) := \max_{r \in \mathcal{M}} |d(p, r) + d(r, p) - d(q, r) - d(r, q)|.$$

**Definition 58.** [20] *A Lorentz space is a pair  $(\mathcal{M}, d)$  where  $\mathcal{M}$  is a set and  $d$  a Lorentz distance function such that  $(\mathcal{M}, D)$  is a compact metric space.*

Then we can define an approximate, or  $\epsilon$ -isometry by the following.

**Definition 59.** [20] *Let  $\epsilon$  be a positive real number. Then a map  $f : \mathcal{M} \rightarrow \mathcal{M}$  is an  $\epsilon$ -isometry if it changes the distance (according to the Lorentz distance function) between points by no more than  $\epsilon$ , that is*

$$|d(f(x), f(y)) - d(x, y)| < \epsilon.$$

We should take great care to note that Noldus and Bombelli define the approximate isometry in [20] on a single manifold, as a map from the manifold to itself. A generalization would be needed if one hopes to consider  $\epsilon$ -isometries

between two distinct manifolds, as one must in the *hauptvermutung* of Causal Set Theory.

However, there is also a great relaxing of the requirements which this isometry must meet, when compared with the rough description set forth in the foundational paper [18], which requires an approximate isometry to be a diffeomorphism. As discussed in the previous chapter, the smoothness required of a diffeomorphism makes it quite difficult to map  $\mathcal{M}_1$  diffeomorphically to  $\mathcal{M}_2$  due to the excision in  $\mathcal{M}_2$ .

The relaxed definition given above (which we note is due to one of the same authors as the original paper [18]) does not ask that the approximate isometry  $f$  meet any smoothness requirements. The definition works for any map  $f$  which satisfies the  $\epsilon$ -distance preserving condition.

Let us recall our discussion in section 7.2.2, regarding  $\mathcal{M}_1$  and  $\mathcal{M}_2$ . The main idea was that any path in  $\mathcal{M}_1$  which may traverse the single-point excision in  $\mathcal{M}_2$  can be deformed an arbitrarily small amount in order to dodge the excision. The distance between two points in  $\mathcal{M}_2$  thus need not differ by more than an arbitrarily small amount from the distance between the same points in  $\mathcal{M}_1$ .

While it is tempting to say that  $\mathcal{M}_1$  and  $\mathcal{M}_2$  are  $\epsilon$ -isometric according to definition 59, we would need to generalize the definition of an  $\epsilon$ -isometry to be a map between two different manifolds.

## 8.2 A Lorentzian Generalization of Euclidean Isometries

In his paper, [19], Noldus explores generalizing the Ascoli-Arzelà Theorem. The Ascoli-Arzelà theorem is canonically set in Euclidean metric spaces and concerns the convergence of families of real functions. This theorem provides a powerful result for determining isometry between Euclidean metric spaces. Noldus was interested in generalizing the Ascoli-Arzelà Theorem to obtain a tool to determine isometries between spacetimes. This may provide a helpful new means to explore the *hauptvermutung* of Causal Set Theory, if we can apply Noldus' result to determine whether spacetimes which admit the same faithfully embedded causal set are isometric, in agreement with the *hauptvermutung*.

The culminating result of this section may help where the previous one concerning  $\epsilon$ -isometries could not. The generalization of the Ascoli-Arzelà theorem is aimed at identifying two *distinct* Lorentzian manifolds as isometric. This is different from the  $\epsilon$ -isometry of section 8.1 which was technically only defined on a single manifold. Of course, this leaves the challenge of making the generalized Ascoli-Arzelà theorem “approximate” in the sense of the *hauptvermutung*.

We need a few more definitions in order to understand Noldus' work.

**Definition 60.** *A family of functions,  $\{f_n\}_{n \in \mathbb{N}}$  defined on a set  $E$  in a metric*



space  $X$  is equicontinuous if,  $\forall \epsilon > 0$ , there is a  $\delta > 0$  such that

$$d(x, y) < \delta \Rightarrow |f_n(x) - f_n(y)| < \epsilon,$$

$\forall x, y \in E$  and  $\forall n \in \mathbb{N}$ .

**Definition 61.** A metric space  $X$  is said to be complete if every Cauchy sequence converges.

We recall that Cauchy sequence is a sequence  $\{p_n\}$  for which, given any  $\epsilon > 0$ , there is an integer  $N$  such that if  $n, m \geq N$ , then  $d(p_n, p_m) < \epsilon$ .

**Definition 62.** A sequence of functions  $\{f_n\}$  defined on a set  $E$  in a metric space  $X$  is said to converge uniformly to a function  $f$  if, given any  $\epsilon > 0$ , there exists an integer  $N$  such that

$$n \geq N \Rightarrow |f_n(x) - f(x)| < \epsilon,$$

$\forall x \in E$ .

**Definition 63.** A subset  $A$  of a metric space  $X$  is precompact if the closure of  $A$  is compact.

We now turn to Noldus' 2004 paper. Noldus' idea is to construct a Lorentzian analog of the Ascoli-Arzelà Theorem. The Ascoli-Arzelà Theorem in its usual form provides a useful tool for identifying isometries between Euclidean metric spaces. With a Lorentzian version, one may be able to identify isometries between spacetimes applicable to the *haupvermutung* of Causal Set Theory.

In order to state the Ascoli-Arzelà Theorem in the manner applicable to Noldus' strategy, we need a few more specific definitions. In the following,  $(X, d_X)$  and  $(Y, d_Y)$  are compact metric spaces.

**Definition 64.** [19] A map  $f : X \rightarrow Y$  is a bi-Lipschitz map if there exist positive real numbers,  $\alpha, \beta$  such that for all  $x, y \in X$ ,

$$\alpha d_X(x, y) \leq d_Y(f(x), f(y)) \leq \beta d_X(x, y).$$

The minimal such  $\beta$  is termed the dilatation of  $f$ ,  $dil(f)$ . The maximal such  $\alpha$  is the co-dilatation. We can now define the Lipschitz distance as a distance between metric spaces.

**Definition 65.** [19] Let  $\mathcal{H}_L$  denote the space of all bi-Lipschitz homeomorphisms. Then the Lipschitz distance  $d_L$ , between metric spaces  $(X, d_X)$  and  $(Y, d_Y)$  is defined as

$$d_L := \inf_{f \in \mathcal{H}_L} \{ |\ln(dil(f))| + |\ln(dil(f^{-1}))| \}.$$

We now state the Ascoli-Arzelà Theorem.

**Theorem 8.2.1.** [21] *Let  $(X, d_X)$  and  $(Y, d_Y)$  be second-countable, locally compact metric spaces, where  $(Y, d_Y)$  is also complete. Assume that the sequence of functions  $\{f_n\}$ , where  $f_n : X \rightarrow Y \forall n$  is equicontinuous such that the sets  $\bigcup_n f_n(x)$  are bounded with respect to  $d_Y \forall x \in X$ . Then there exists a continuous function  $f : X \rightarrow Y$  and a subsequence of  $\{f_n\}$  which converges uniformly on compact sets of  $X$  to  $f$ .*

We briefly describe reasoning which, following from the Ascoli-Arzelà theorem gives the Euclidean result that

$$d_L(X, Y) = 0 \iff X \text{ and } Y \text{ are isometric.} \quad (8.1)$$

We would seek a sequence of uniformly converging bi-Lipschitz homeomorphisms,  $\{f_n\} \in \mathcal{H}_L$  such that

$$\begin{aligned} \text{dil}(f_n) &\rightarrow 1, \\ \text{dil}(f_n^{-1}) &\rightarrow 1, \\ \text{co-dil}(f_n) &\rightarrow 1 \end{aligned}$$

as  $f_n \rightarrow f$ . This would sandwich

$$d_X(x, y) \leq d_Y(f(x), f(y)) \leq d_X(x, y) \Rightarrow d_X(x, y) = d_Y(f(x), f(y))$$

$\forall x, y \in X$ , as well as return a value of 0 for  $d_L(X, Y)$ .

We now define two more Lorentzian analogs of Euclidean objects.

**Definition 66.** [19] *Given a map between globally hyperbolic spacetimes,  $f : (\mathcal{M}, g) \rightarrow (\mathcal{N}, h)$ , a timelike dilatation of  $f$ , denoted  $\text{tdil}(f)$  is the smallest number  $\beta$  such that*

$$d_h(f(x), f(y)) \leq \beta d_g(x, y) \forall x, y \in \mathcal{M}.$$

**Definition 67.** [19] *A map like  $f$  above is timelike Lipschitz if  $\text{tdil}(f)$  is bounded.*

We can now state Noldus' Lorentzian version of the Ascoli-Arzelà Theorem.

**Theorem 8.2.2.** [19] *Let  $\{f_n\}$ ,  $f_n : (\mathcal{M}, g) \rightarrow (\mathcal{N}, h)$  be a sequence of surjective bi-Lipschitz maps such that  $\bigcup_m f_n(x)$  and  $\bigcup_m f_n^{-1}(y)$  are precompact  $\forall x \in \mathcal{M}, y \in \mathcal{N}$  in  $\mathcal{N}$  and  $\mathcal{M}$  respectively. Let  $\{c_n\}_{n \in \mathbb{N}}$  be a descending sequence converging to 0 such that  $\text{tdil}(f) \leq 1 + c_n$  and  $\text{tdil}(f_n^{-1}) \leq \frac{1}{1 - c_n}$ , then there exists a subsequence  $\{f_{n_k}\}$  of  $\{f_n\}$  such that  $f_{n_k} \rightarrow f$ , where  $f$  is an isometry.*

We now require a theorem concerning the convergence of timelike dilatations before we can state the final analogous result concerning the equivalence between zero-distance of metric spaces and isometry of the spaces.

**Theorem 8.2.3.** [19] *Let  $\{f_n\}$  be as in the previous theorem and let  $\alpha < 1 < \beta$ . Suppose  $\text{tdil}(f_n) \leq \beta$  and  $\text{tdil}(f_n^{-1}) \leq \frac{1}{\alpha}$ . Then there exists a subsequence  $\{f_{n_k}\}$  such that  $f_{n_k} \rightarrow f$  pointwise for some function  $f$ . One also has that  $\text{tdil}(f) \leq \beta$  and  $\text{tdil}(f^{-1}) \leq \frac{1}{\alpha}$ .*

Then we have a condition for isometry amongst Lorentzian manifolds in the style of (8.1), albeit with a causal restriction. We note that it deals with elements of a moduli space of Lorentzian manifolds, reminiscent of Surya’s third statement of the *hauptvermutung*.

**Theorem 8.2.4.** [19] *Let  $(\mathcal{M}, g)$  and  $(\mathcal{N}, h)$  be compact globally hyperbolic spacetimes with boundary. Then*

$$d_L((\mathcal{M}, g), (\mathcal{N}, h)) = 0 \iff (\mathcal{M}, g) \text{ and } (\mathcal{N}, h) \text{ are isometric}$$

We need to be careful about the provisions and limitations of this result. Theorem 8.2.4 does supply a way of identifying two spacetimes as isometric. According to the theorem, the spacetimes are identified as “exactly” isometric, not “approximately” as in the *hauptvermutung*. However, the spacetimes in question must be globally hyperbolic in order for the theorem to apply.

The requirement of global hyperbolicity is quite restrictive, and precludes application of this theorem to two of the three spacetimes,  $\mathcal{M}_2$  and  $\mathcal{M}_3$  from the last chapter. The requirement of global hyperbolicity seems to come from the fact, which Noldus does not prove in the paper under consideration, that global hyperbolicity is equivalent to the continuity of the canonical Lorentz distance function.

The theorem does, however, involve an isometry between two distinct spacetimes, which the  $\epsilon$ -isometry of the last section did not. The identification of isometry between different manifolds is a crucial aspect of the *hauptvermutung*.

In the final chapter, we consider whether a connection between the two results outlined here, concerning  $\epsilon$ -isometries on a single spacetime, and exact isometries between different spacetimes, could be integrated into a single tool which might help to give us a more precise formulation of the *hauptvermutung* of Causal Set Theory.

## Chapter 9

# Conclusions and Future Work

Our question in this dissertation has been to examine for which rungs of the causal ladder does the *hauptvermutung* of Causal Set Theory hold.

We first approach an answer by example, using the sample spacetimes of chapter 7. Given the provisional definition of an approximate, or  $\epsilon$ -isometry in the previous chapter, we consider whether the spacetimes of chapter 7 –  $\mathcal{M}_1$ ,  $\mathcal{M}_2$ , and  $\mathcal{M}_3$  – present any contradiction to the *hauptvermutung*.

If Noldus and Bombelli’s  $\epsilon$ -isometry can be generalized to a map between two different manifolds, then these two spacetimes seem to be approximately isometric. The potentially problematic area of  $\mathcal{M}_2$  would be around the single-point excision. However this excision does not have any length. If one were interested in measuring the distance between two points around this excision with either a canonical Lorentz distance function or a Lorentz metric, the path joining the two points could be made arbitrarily small. This suggests that an  $\epsilon$ -isometry between  $\mathcal{M}_1$  and  $\mathcal{M}_2$  could indeed be found. The distance between two points near the excision could be made arbitrarily small as required. Now we recall that these manifolds gave rise to identical causal sets when embedded at a density of  $\rho = 10$ . So all appears to be in order for these two sample spacetimes: the same causal set is faithfully embedded in them, and they are approximately isometric, or comprise the same “essentially unique” manifold. So the *hauptvermutung* seems to hold in the case of  $\mathcal{M}_1$  and  $\mathcal{M}_2$ .

Consider now  $\mathcal{M}_1$  and  $\mathcal{M}_3$ . By the standards of an  $\epsilon$ -isometry, these two spacetimes are not the same. For two points on opposite sides of the excision in  $\mathcal{M}_3$ , there is indeed a minimum length associated to the path joining them, which is a length greater than that of a straight line joining them. By this reasoning,  $\mathcal{M}_1$  and  $\mathcal{M}_3$  are not  $\epsilon$ -isometric. This can be seen in 9.1 below.

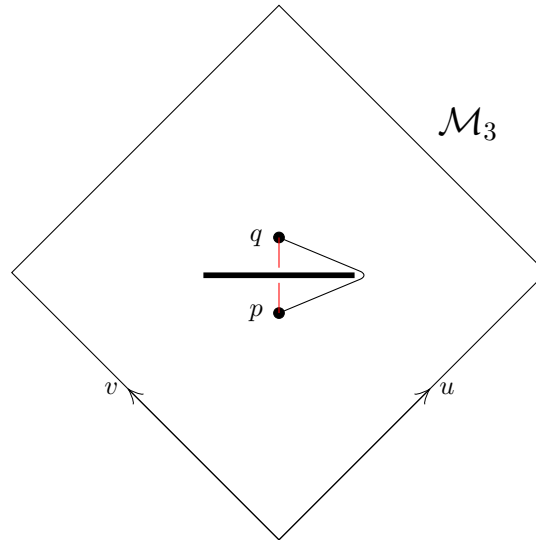


Figure 9.1: Not only would attempting to join the points  $p$  and  $q$  with a length-minimizing curve violate causality, but there is a minimum length associated to a curve which can join the points  $p$  and  $q$ .

Since  $\mathcal{M}_1$  and  $\mathcal{M}_3$  do not permit the same faithfully embedded causal set, these two spacetimes are in agreement with the *hauvermutung* (a contrapositive, where different causal sets are faithfully embedded in two spacetimes which are not “essentially unique”).

With our provisional definition of an  $\epsilon$ -isometry, we can say that a comparison of the three spacetimes in this paper,  $\mathcal{M}_1$  with  $\mathcal{M}_2$  and  $\mathcal{M}_1$  with  $\mathcal{M}_3$  leads to no contradiction of the *hauvermutung*.

As we have discussed, we need to be careful in interpreting the work of Noldus and Bombelli on approximate isometries. The domain and codomain of the  $\epsilon$ -isometry they define are the same.

To determine whether a generalization of the approximate isometry is well-defined for a map between two different manifolds would be a precursor for future work. An interesting strategy might be to search for a junction with the Lorentzian version of the Ascoli-Arzelà Theorem which Noldus has proven in [19]. The goal here would be to arrive at a syncretic result which

- provides a mean for determining  $\epsilon$ -isometry in the style of theorem 8.2.4 (as opposed to “exact” isometry)
- allows for the isometry in this theorem to be a map between *distinct* manifolds (rather than a map defined on a single manifold as Bombelli and Noldus’  $\epsilon$ -isometry)
- holds for spacetimes on any rung of the causal ladder.

The first and second items above ask for an “approximate” version of theorem 8.2.4. The third item asks that the condition of global hyperbolicity be relaxed. If such a result were reached, which connected the  $\epsilon$ -isometry with theorem 8.2.4 and functioned on any rung of the causal ladder, it could yield a powerful mechanism for evaluating the validity of the *hauptvermutung*.

Let us consider again what causal restrictions must be applied to a spacetime in order for the *hauptvermutung* of Causal Set Theory to hold. We are given some clues about what rung we must occupy for the *hauptvermutung* to hold. These clues come from the sample spacetimes of chapter 7 as well as from Noldus’s work on approximate Lorentzian geometry and the Lorentzian Ascoli-Arzelà theorem.

The sample spacetimes of  $\mathcal{M}_1$ ,  $\mathcal{M}_2$ , and  $\mathcal{M}_3$  all resided between strong causality and global hyperbolicity. Recall that  $\mathcal{M}_1$  was globally hyperbolic,  $\mathcal{M}_2$  was causally continuous, and  $\mathcal{M}_3$  was stably causal. All three manifolds were of course strongly causal since these rungs lie above strong causality on the causal ladder. They presented no contradiction to the *hauptvermutung*.  $\mathcal{M}_1$  was provisionally deemed approximately isometric to  $\mathcal{M}_2$ , and they permitted the same faithfully embedded causal set.  $\mathcal{M}_1$  was deemed not approximately isometric to  $\mathcal{M}_3$ , and when the same causal set elements were sprinkled in  $\mathcal{M}_1$  and  $\mathcal{M}_3$ , their causal relations were different, and thus the two spacetimes gave rise to *different* causal sets. The findings from the sample spacetimes seem to demonstrate that the *hauptvermutung* holds on rungs above strong causality. At least by the example of these three sample spacetimes, rungs above strong causality seem to be a safe place to assume the verity of the *hauptvermutung*.

The results of Bombelli and Noldus concerning Lorentzian isometries all function between the same rungs as the ones in which the sample spacetimes resided. In particular, global hyperbolicity was required for the Lorentzian analog of the Ascoli-Arzelà theorem. Additionally, the strong metric defined by Noldus also requires a Lorentz distance function that is continuous in the Alexandrov topology. As was proven in chapter 3, the Alexandrov topology agrees with the manifold topology exactly when the spacetime is strongly causal. So on a strongly causal spacetime, the strong metric Noldus requires would be continuous on the manifold topology as well. This suggests that strong causality might provide a suitable setting to work with the strong metric and use the associated results. These findings suggest that the rungs of strong causality and/or global hyperbolicity might be important for the *hauptvermutung* to hold true.

We cannot make concrete statements, since the  $\epsilon$ -isometries and the Lorentzian Ascoli-Arzelà theorem require some modification in order to be applied to our question. We recall that these entail generalizing the  $\epsilon$ -isometry to be a map between distinct manifolds and loosening the Lorentzian Ascoli-Arzelà to a result concerning approximate isometry. It is unclear what effect these alterations would have on the provisions of these results.

A strategy for altering Noldus and Bombelli’s results would be an interesting line of future work. Especially important would be to understand for which rungs of the causal ladder these results hold, after the results are altered in

the ways mentioned above. On the one hand altering theorem 8.2.4 to make it approximate may allow us to lower the rung on the causal ladder where the result holds. On the other, we need to generalize the  $\epsilon$ -isometry to be a map between distinct manifolds, which may require a stricter causal condition to preserve the definition. We hope to explore what the causal implications of these alterations would be.

Examining the validity of the *haupvermutung* on rungs of the causal ladder below strong causality would also be crucial. While rungs below the causal ladder were discussed, we did not explore the validity of the *haupvermutung* on rungs strictly below strong causality. In addition, the results concerning approximate isometry all seem to function on rungs at or above strong causality. This leaves the rungs below strong causality relatively unexplored. This must be ameliorated in future work in order to develop a more robust understanding of the *haupvermutung*. As well as examining spacetimes with different causal structures, Poisson sprinklings with different, and preferably higher densities must also be tested. Of particular focus should be testing the prediction of the limiting behavior of the ratio of the expected number of blocked causal relations in  $\mathcal{M}_3$  to the expected number of causal relations in  $\mathcal{M}_1$ . With higher density sprinklings, we might test whether

$$\lim_{l \rightarrow \sqrt{2}} \frac{\langle N(BR) \rangle}{\langle N(R) \rangle} = \frac{2}{3}$$

holds true.

If Causal Set Theory continues to progress, confidence in the *haupvermutung* may grow as experiments and further theoretical work confirm its verity. The community studying it may then begin to accept the validity of the *haupvermutung* even without a formal proof. In the meantime however, it will be important to continue scrutinizing this central conjecture, alongside other work in Causal Set Theory.

# References

- [1] Hartland S. Snyder. Quantized space-time. *Phys. Rev.*, 71:38–41, Jan 1947.
- [2] A. Schild. Discrete space-time and integral lorentz transformations. *Phys. Rev.*, 73:414–415, Feb 1948.
- [3] E. L. Hill. Relativistic theory of discrete momentum space and discrete space-time. *Phys. Rev.*, 100:1780–1783, Dec 1955.
- [4] Riemann B. On the hypotheses which lie at the bases of geometry. *Nature*, VIII(14–17):36, 37, 1873.
- [5] Alfred A. Robb. A theory of time and space. *Mind*, 24(96):555–561, 1915.
- [6] Walter Rudin. *Principles of mathematical analysis*. McGraw-Hill Book Company, Inc., New York-Toronto-London, 1953.
- [7] E. H. Kronheimer and Roger Penrose. On the Structure of causal spaces. *Proc. Cambridge Phil. Soc.*, 63:481–501, 1967.
- [8] E. C. Zeeman. Causality implies the lorentz group. *Journal of Mathematical Physics*, 5(4):490–493, 1964.
- [9] E Minguzzi. The causal ladder and the strength of  $k$ -causality: II. *Classical and Quantum Gravity*, 25(1):015010, dec 2007.
- [10] Roger Penrose. *Techniques in Differential Topology in Relativity*. Society for Industrial and Applied Mathematics, 1972.
- [11] E. Minguzzi and M. Sanchez. The causal hierarchy of spacetimes. 2006.
- [12] S. W. Hawking and G. F. R. Ellis. *The Large Scale Structure of Space-Time*. Cambridge Monographs on Mathematical Physics. Cambridge University Press, 1973.
- [13] S W Hawking, A R King, and P J McCarthy. A new topology for curved space-time which incorporates the causal, differential, and conformal structures. *J. Math. Phys. (N.Y.)*, v. 17, no. 2, pp. 174-181, 17(2), 2 1976.



- [14] David B. Malament. The class of continuous timelike curves determines the topology of spacetime. *Journal of Mathematical Physics*, 18(7):1399–1404, 1977.
- [15] Onkar Parrikar and Sumati Surya. Causal topology in future and past distinguishing spacetimes. *Classical and Quantum Gravity - CLASS QUANTUM GRAVITY*, 28, 02 2011.
- [16] David Finkelstein. Space-time code. *Phys. Rev.*, 184:1261–1271, Aug 1969.
- [17] Sumati Surya. The causal set approach to quantum gravity. *Living Reviews in Relativity*, 22(1), sep 2019.
- [18] Luca Bombelli, Joochan Lee, David Meyer, and Rafael D. Sorkin. Space-time as a causal set. *Phys. Rev. Lett.*, 59:521–524, Aug 1987.
- [19] Johan Noldus. A lorentzian gromov–hausdorff notion of distance. *Classical and Quantum Gravity*, 21:839, 01 2004.
- [20] Luca Bombelli and Johan Noldus. The moduli space of isometry classes of globally hyperbolic spacetimes. *Classical and Quantum Gravity*, 21, 03 2004.
- [21] K. Yosida. *Functional Analysis*. Classics in Mathematics. Springer Berlin Heidelberg, 2012.